A NOVEL AND SUSTAINABLE SYNTHESIS OF 2D GRAPHENE QUANTUM DOTS

Lappeenranta–Lahti University of Technology LUT
Master's degree program in Chemical engineering, Master's thesis
2022
Kai Alfred Viinanen
Examiner(s): Professor, Mika Mänttäri
Postdoctoral Researcher, Kinga Skalska

ABSTRACT

Lappeenranta–Lahti University of Technology LUT
LUT School of Engineering Science
Chemical Technology

Kai Alfred Viinanen

A Novel and Sustainable Synthesis of 2D Graphene Quantum Dots

Master's thesis
2022
60 pages, 34 Figures, 8 tables
Examiner(s): Professor, Mika Mänttäri and Postdoctoral Researcher, Kinga Skalska

Keywords: Graphene quantum dots, GQDs, synthesis, optimal conditions, microwave irradiation

Graphene quantum dots (GQDs) have lately gained big interest due to their unique properties and possible applications. This unique component can be synthesized via bottom-up and top-bottom approaches using precursors that are cheap, ecological, and easy to obtain.
This work aims to find the most optimal conditions to produce controllable GQDs of wanted size ecologically and economically by studying how different compositions, used temperatures/irradiation, and reaction times affect synthesis.
It was found that the presence of water produces fewer by-products and more GQDs in quantity but with a smaller average size. In addition, it was found that Catalyst compensates for the presence of water by producing GQDs with bigger average size, but it needs to be in a very small amount otherwise synthesis will go out of control.

TIIVISTELMÄ

Lappeenrannan–Lahden teknillinen yliopisto LUT
LUT Teknis-luonnontieteellinen
Kemiantekniikka

Kai Alfred Viinanen

Uusi ja Kestävä 2D-grafeenikvanttipiste Synteesi

Kemiantekniikan pro gradu -tutkielma
2022
60 sivua, 34 kuvaa ja 8 taulukkoa
Tarkastaja(t): Professori, Mika Mänttäri ja Tutkijatohtori, Kinga Skalska

Avainsanat: Grafeenikvanttipisteet, GQDs, synteesi, optimaaliset synteesi olosuhteet, mikroaaltouuni säteilytys

Grafeenikvanttipisteet (GQDs) ovat viime aikoina herättäneet suurta kiinnostusta niiden ainutlaatuisten ominaisuuksien ja mahdollisten sovellusten vuoksi. Tämä ainutlaatuinen komponentti voidaan syntetisoida alhaalta ylöspäin sekä ylhäältä alaspäin suuntautuvalla lähestymistavalla käyttämällä halpoja, ekologisia ja helposti hankittavia raaka aineita.
Tämän työn tavoitteena on löytää optimaaliset olosuhteet, jotta halutun kokoisten GQD:iden tuottaminen olisi kontrolloitua, ekologista sekä taloudellista, tutkimalla miten raaka aineen koostumus, käytetty reaktio lämpötila/säteilytys sekä reaktioaika vaikuttavat GQD:iden syntetisointiin.
Tuloksista voi huomata, kuinka veden läsnäolo vähentää sivureaktioita ja tuottaa enemmän GQDs, mutta syntetisoidut GQDs omaavat pienemmän koon. Tämän lisäksi voi huomata kuinka katalyytti kompensoi veden vaikutuksen tuottamalla suuremman kokoisia GQDs, mutta katalyyttiä on lisättävä pienissä määrin, muuten synteesi muuttuu kontrolloimattomaksi.

SYMBOLS AND ABBREVIATIONS

Roman characters

h	Time	[hour]
g	Mass	[gram]
m-%	Mass ration	[-]
W	Watt	[J/s]

Abbreviations

CA	Citric acid
CFs	Carbon fibers
CQDs	Carbon quantum dots
CVD	Chemical vapor deposition
NaOH	Sodium hydroxide
DMF	Dimethylformamide
DMSO	Dimethyl sulfoxide
Da	Dalton
F	Fluorine
GQDs	Graphene quantum dots
GO	Graphene oxide
H^+	Hydrogen ion
MWCO	Molecular weight cut-off
N	Nitrogen
NH_3	Ammonia
N-GQDs	Nitrogen dopped GQDs
NPs	Nanoparticles
P	Phosphor
PL	Photoluminescence
QDs	Quantum dots
QY	Quantum yield
RGO	Reduced graphene oxide
SQDs	Semiconductor quantum dots
S	Sulphur

SEC	Size exclusion chromatography
SP	Stationary phase
TMB	3,3,5,5-tetramethylbenzidine
TEM	Transmission Electron Microscopy

Table of contents

1 Introduction

Graphene quantum dots (GQDs) are conventionally synthesized using oil, petroleum coke, coal, fossils as well as other carbonaceous materials but on the negative side synthesis routes that use earlier mentioned precursors often need strong acids and/or organic solvents and temperature so that reaction could start or that it will react in a wanted way. These severe conditions result in a fast corrosion of set-up equipment as well as intensive energy usage which cannot be called an effective, biosafe, non-toxic, economical, or green synthesis method.

It is known that the properties of GQDs derive from both quantum dots (QDs) and graphene making it close to being unrivaled because of possible applications. It is a result of the few-layered crystalline structure, more abundant edge sites, and smaller size. Mansuriya et al. (2019) and Younis et al. (2020) have reported that produced GQDs will have different features depending on what synthesis method, precursor, composition, and experimental conditions are selected because features are easily tunable in optimized conditions [1,2].

In recent years it has been studied how to exploit renewable resources, ranging from simple and natural molecules to complex compounds such as wood charcoal, coffee ground, different wastes, manure, processing residue, and many more, to obtain biomass-derived GQDs and stop using unrenewable raw materials and increase energy security and environmental safety by making use of both top-down and bottom-up approaches.

GQDs depending on size, functionality, and shape have many different characteristics which give a wide range of applications such as the medical field to remove cancer or wastewater treatment to remove microplastics, pharmaceuticals, and fertilizers (phosphor). This study focuses on finding the most optimal conditions and composition to produce effective, biosafe, non-toxic, economical, and green GQDs of different sizes by utilizing ecological and cheap raw materials such as Citric acid (CA) (a weak organic acid) and D(+)-glucose (a carbohydrate). The reason why these precursors are chosen is that both are available in nature and are the most popular carbon precursors used in many articles, because of their biocompatibility, low cost, and ease of supply.

2 Theoretical Part of Graphene Quantum Dots

To understand why GQDs are gaining interest, it is important to familiarize ourselves with the unique characteristics of GQDs. That is why the next chapters will describe in detail what GQDs are, how they behave, how pristine and modified properties can affect their different applications and different methods to obtain/synthesize them as well as the good and bad sides of these methods.

2.1 GQDs as Component

It is said that GQDs are a new member of the carbon material family that was first discovered in 2010 when graphene sheets were put through acid etching and as a result produced GQDs. Not long after that, it was found that GQDs have superior characteristics and are less toxic compared with conventional semiconductor quantum dots (SQDs). Even if GQDs consist of carbon elements and are small fragments of graphene their properties derive from both QDs and graphene. Younis et al. (2020) explained it as being a result of a tuneable bandgap that can be further tuned by edge effect and quantum confinement [2]. In a sense, it can be said that the predecessor of Graphene Quantum Dots GQDs is Carbon Quantum Dots (CQDs). They both consist of the same carbon element and their structure resembles each other. But while CQDs are characteristically quasi-spherical carbon nanoparticles composed of amorphous to crystalline carbon base, the GQDs consist of a few (1-3) layered graphitic crystalline structures which make GQDs more compact. The structural difference between CQDs and GQDs are illustrated in Figure 1.

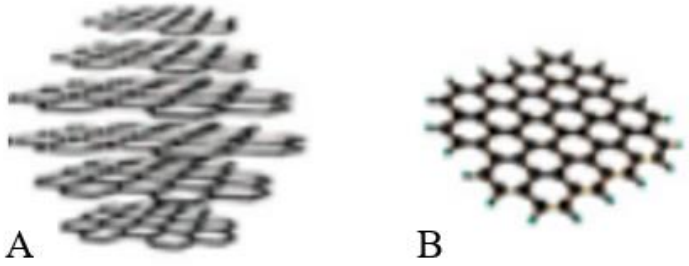

Figure 1. Difference between CQDs (A) and GQDs (B) [3]

Mansuriya et al. (2019) and Younis et al. (2020) mentioned that because of the few-layered crystalline structure, GQDs have more abundant edge sites, smaller size/larger specific surface, and higher crystallinity than CQDs [1,2]. Therefore, GQDs were classified as a new category of Quantum Dots/carbon material family with their tuneable optical, electrical, chemical, and structural properties such as their high solubility, intercity, chemical stability/environmentally friendly, low toxicity, easy-to-be-functionalized with organic, biological, or inorganic molecules, excellent photoluminescence (PL) property, biocompatibility, robusticity, photo-stability and photo-bleaching [1].

2.1.1 Introduction to Different Applications of GQDs

These physicochemical properties of GQDs, which were mentioned in the previous chapter, give a wide range of potential applications from environmental to biological. Campuzano et al. (2019) state that the edge effect (which also affects electrical conductivity and makes GQDs highly soluble) and quantum confinement make it possible to have high-speed electron transport/movement in GQDs [4,5]. Because of the aromatic structure, their small size, and high-speed electron movement GQDs have peroxidase mimetic activity making them good material in sensing other components and elements followed by adsorption. Singh et al. (2018) mentioned that QDs, especially GQDs, are good at sensing and reducing H_2O_2 which as result accelerates •OH radical generation and can further oxidate other components such as 3,3,5,5-tetramethylbenzidine (TMB) [5]. In addition, because of these electrochemical properties, GQDs are used to design novel electrode materials in the field of supercapacitors, photovoltaic cells, and fuel cells. Also because of their chemical stability, low toxicity, biocompatibility, ease to be functionalized with organic, biological, or inorganic molecules, and excellent PL properties GQDs can be applied in the biomedical field. For example, GQDs can be used as drug delivery and/or bio-imaging compound. However, the widespread use of GQDs is hindered by the poor understanding of their PL mechanisms [6].

2.1.2 GQDs and Their Photoluminescence

One of the most interesting properties that GQDs have is their PL. It has been reported that GQDs are effective in photon-harvesting in short-wavelength around 260 nm to 390 nm region because of π−π transition of C=C bonds and n-π transition of C=O. It is also a known fact that GQDs can emit wavelengths around the whole spectrum of visible light. Depending on the synthesis method and precursors, GQDs can have different particle sizes ranging between 1 to 100 nm while their forms can be triangular, elliptical, hexagonal, or/and quadrate. To date, it is known that the PL of GQDs can be tuned by their size, edge configuration, shape, attached chemical functionalities, heteroatom doping, and defects.

Another interesting thing about these nanometre-sized materials is that they have size-dependent photophysical properties originating from the quantum confinement effect. However, according to Fu et al. (2007), the PL of a heterogeneously hybridized carbon network is essentially determined by the embedded small sp2 clusters isolated by sp3 carbons [6]. Whereas Bailey et al. (2003) suggested that fluorescence of GQDs occurs by defect state emission and/or intrinsic state emission (e.g., quantum size, recombination of localized electron-hole pairs, zigzag edge sites) [7]. This means that increase in the size of GQDs will result in the growth of absorption and emission wavelength. The reason behind the size-dependent PL phenomenon is the decrease of bandgap which results from π-electron delocalization. Efros et al. (1996) stated that various spherical semi-conductors of the QDs family have similar size-dependent emission phenomena but GQDs are much more promising because of their few layered structures. So, if the specific wavelength that GQDs can emit is wanted then it means that GQDs need to be with specific shape and size. To achieve that we need to choose a synthesis method and precursors which can give us controllable GQDs synthesis.

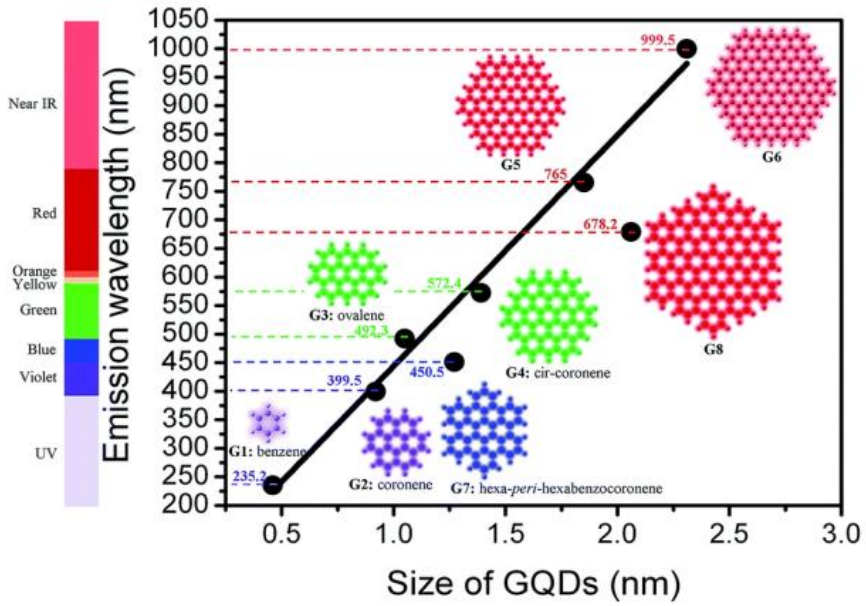

Figure 2. Emission wavelength dependence based on GQDs size [8]

If initial carboxyl and/or epoxy groups in GQDs will be modified or reduced, then it will result in the promotion of intrinsic state emission which may change the π-π electron of sp^2 domain energy gaps. In other words, it can change the PL of GQDs by tuning quantum confinement. The tuning of quantum confinement can be done through sp3 and sp2 configuration, size, shape, heteroatom doping, attached chemical functionalities, and defects [9,10]. It is speculated that (OH) groups suppress defect state emission and nonradiative emission because defects in GQDs are reduced. Heteroatom doping of GQDs brings many benefits to the usability of GQDs. It is discovered that doping of heteroatom such as nitrogen (N) is effective at enhancing PL properties of GQDs depending on doping ratio (%) because the difference in excited states lowers the energy needed to produce PL as well as PL emitted wavelength [2,11].

Functionalization works with the same principle as heteroatom doping of the GQDs. Surface functionalization of GQDs is performed using electron-donating or electron-withdrawing groups which make it possible for GQDs to be reduced or oxidized in solution. With this, it is possible to further tune the bandgap (distance of the state from where electrons drop to the ground state) while producing a large variety of functionalized GQDs with different characteristics. Theoretically, this brings many benefits and possible applications. It is interesting fact that GQDs, functionalized by ammonia (NH_3), can have different PL effects depending on pH. Meaning that the PL of GQDs changes with pH, because of the ammonia's ability to lose or gain hydrogen ion (H^+) (protonation and deprotonation) which affects the

bandgap/excited state [12,13]. For example, the potential application of the GQDs features to sense pH and absorb pollutants could be used in wastewater treatment. Because in this case, GQDs will not only tell what pH is but also act as an adsorbent that will lose its PL property with the adsorbed pollutants.

2.1.3 Intensity of Photoluminescence

In addition to PL properties, GQDs have tuneable fluorophore signals as well as intensity (brightness). This can be affected by quantum yield (QY) which is defined as the ratio of the number of emitted photons divided by the number of absorbed photons. Zhu et al. (2011) said that photoluminescence quantum yields (PLQY) of pristine GQDs are somewhere from 4% to 11% depending on the synthesis method [14]. It was discovered that doping GQDs by moieties or additional electrons enhances the intensity of fluorescence. In other words, the reason behind poor QY is due to the emissive traps on the **surface** and the **local electronic environmen**t. That is why the surface passivation layer is necessary to improve their intensity.

Nitrogen-doped GQDs (N-GQDs) have enhanced PL intensity and lower toxicity than pristine GQDs. Ju et al. (2014) reported that the stronger PL intensity of N-GQDs was the result of QY which had grown from an initial 4.8% to 23.3% [15]. Also, it is mentioned that co-doping GQDs can further enhance their PL intensity. Kundu et al. (2015), Jie Zhang et al. (2015), and Zaicheng Sun et al. (2015) have mentioned that co-doping N-GQDs with sulfur (S), fluorine (F), and phosphor (P) has positive effects in the PL intensity of GQDs enhancing it by 61%, 70%, and 53% respectively [16–18]. Co-doping with heteroatoms can contain extensive delocalized π-electrons.

The doping of GQDs by heteroatom will decrease their PL lifetime. The lifetime of fluorescence means the time that fluorophore emits the photon by dropping electron to the ground state through decay that can be nonradiative or radiative which can be affected by polarity, microenvironment, ionic strength, temperature, viscosity, local pH, and conjugated molecules. In other words, this can be explained by the Jablonski diagram where S_1 and S_0 states can be modified by doping of GQDs making absorption, non-radiative transition, and fluorescence process faster. Jablonski's diagram is shown in Figure 3.

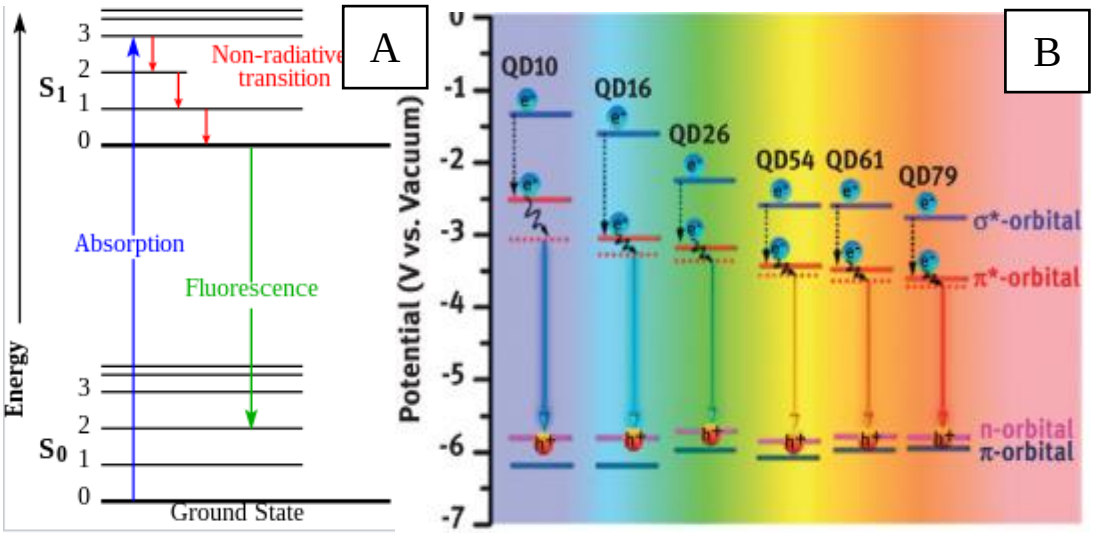

Figure 3. Jablonski diagrams where (A) illustrate absorption, non-radiative transition, and fluorescence process [19] while (B) illustrates how states affect PL wavelength [8]

Tang et al. (2014) reported that they tested N-GQDs of different sizes to understand the size dependence of the PL decay at its fixed peak wavelengths of excitation (375 nm) and emission (570 nm). They found that the PL of larger N-GQDs decays faster and suggested that the presence of nitrogen, after absorption of UV-VIS light, will accelerate the number of emitted photons. The drawback of heteroatom doping is that the PL intensity over time will decrease faster than without heteroatom doping. For example, pristine GQDs will show bright PL even after 3 months, if they are stored in optimal conditions, while N-GQDs can last on average for 1 month in optimal conditions. The reason that the PL intensity of N-GQDs does not last long is that N-GQDs generate reactive oxygen species in higher amounts than pristine GQDs which the result will degrade the structure of N-GQDs [20].

2.2 Synthesis Categories

Nowadays synthesis of any chemical or compound can be divided into two main categories which are bottom-up and top-down approaches. Each of the categories has its raw materials used in synthesis, advantages, and disadvantages which are listed in Table 1.

Table 1. Comparison of bottom-up and top-down approach for GQDs

	Bottom-up approach	Top-down approach
Precursor	Organic molecules	Graphite sheets & nanotubes
Processing method	Physical and Chemical	Physical
Temperatures (°C)	~ 200 to 400	~ 800 to 1400
Advantages	Cheap Controllable	Large scale production No purification
Disadvantages	Large-scale production is difficult Chemical purification needed Aggregation	Broad size distribution Different particle shapes Hard to control Expensive

The bottom-up approach is more restricted because only a few methods can be used to successfully produce GQDs while the top-down can utilize all synthesis methods to produce GQDs. Table 2 summarizes methods that can be used to synthesize GQDs and the categories to which these methods are related.

Table 2. Synthetic methods and their category

Methods	Category	
	Bottom-up approach	Top-down approach
Hydrothermal	x	x
Solvothermal	x	x
Pyrolysis	x	x
Microwave-assisted	x	x
Electrochemical Exfoliation	-	x
Acid Etching	-	x
Ultrasonication Exfoliation	-	x
Lithography Process	-	x
Chemical Exfoliation	-	x

2.2.1 Bottom-Up Synthesis of GQDs

The bottom-up method uses atomic or molecular precursors for carbon sp2 controllable synthesis from organic polymers (such as styrene) or carbonization of organic molecules (such as citric acid) to form an organic compound which in our case is GQDs. In other words, the bottom-up method can produce homogeneous, and high-quality GQDs via rigid synthetic chemistry. Thus, this method has an advantage in better structural and size control, purity, morphology, and properties of GQDs. Because of these advantages, bottom-up synthesized GQDs have many applications, mostly in medicine/biology, but it also has their disadvantages such as the need for special precursors and complex synthetic routes while GQDs have low solubility and a strong tendency toward aggregation [21]. Manikandan et al. (2019) mentioned that this method is very difficult because of the aggregation that interacts with the aromatic molecule's edges (surface interactions that can form many-layered structures) [21]. To solve this problem the edges are decorated for example, with phenyl groups via covalent bonding. As the result, it forms 3D cages that surround the moieties of graphene which increase the distance between each layer while improving the solubility of larger GQDs.

2.2.1.1 Thermal Heating Processes

The most used bottom-up approach to synthesize GQDs is the carbonization of organic precursors such as glycerol, L-glutamic acid, CA, ascorbic acid, coffee grounds, and many more via heating using pyrolysis (inert gas present), or thermal processes (oxygen present). The thermal process can be defined as hydrothermal and solvothermal. The thermal method is a green/ecological method where chemicals/materials are mixed and put into an autoclave which is then moved inside the oven for heating. The pyrolysis method is done in the same way as the thermal method, but the difference is in the autoclave because compared to the thermal method, where oxygen is present, the pyrolysis method needs inert gas such as nitrogen which needs to be led into the autoclave [21]. The principle of these methods is the same because in the carbonization process organic molecules are condensed by heating them above their melting points. This further stimulates the nucleation of organic molecules which in the end form GQDs. Manikandan et al. (2019) stated that the carbonization process is not only simple but also cost-effective where many different precursors can be used while produced GQDs are uniform in size and have mostly single layers [21]. But on the other hand, even if raw materials and the method themselves are cheap and easy to use, the energy efficiency and large-scale production are not at a satisfactory level. The reason why energy effectiveness is low is that the conventional heating process takes from 4 to 24 hours. If the used heating time is compared to small amounts of gain product, then low energy-effectiveness can be seen. Figure 4 is an illustration of the carbonization process using thermal heating.

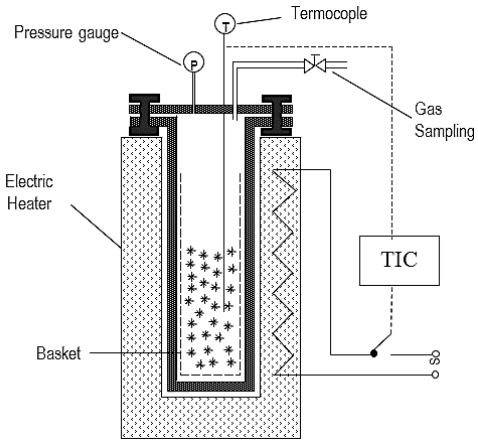

Figure 4. Closed vessel of thermal treatment batch process [22]

2.2.1.2 Microwave Irradiation Process

Instead of a simple thermal process, many processes can be done with a microwave irradiation process. Because microwave irradiation affects bonds directly the heating is homogenous and fast, it can improve yield, and the product's purity, as well as reaction time, can be shortened [21]. For example, 1 min microwave irradiation under 700W can give the same results as 4-8 hours of thermal treatment under 180 °C. The reason why thermal heating is ineffective is that the thermal method first affects the vessel by warming it through convection after which heat is conducted through the vessel's walls into solution followed by heat energy transfer to the molecular bonds. The illustration of convectional and radiational heating can be seen in Figure 5.

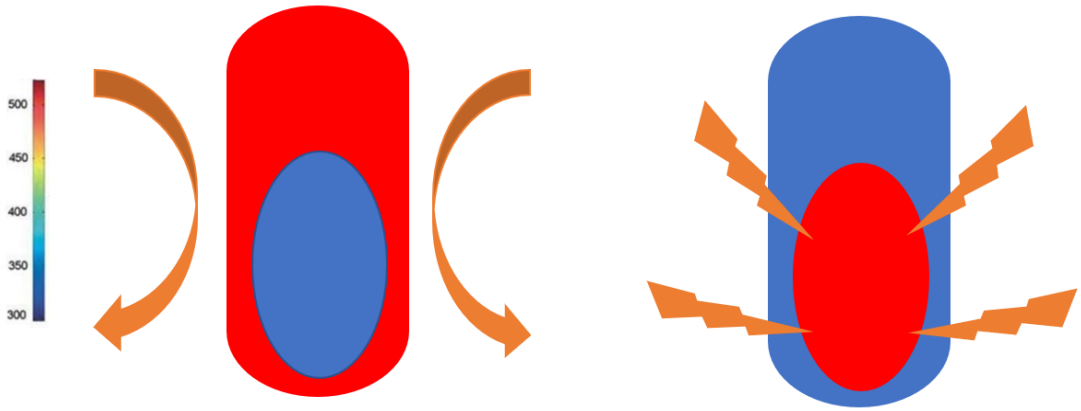

Figure 5. Convectional and radiational heating illustration

On one side the implementation of the microwave method can be expensive. But on the other side, the energy consumption is much smaller than in the conventional thermal process. An industrial microwave-integrated heating system used for fast heating to evaporate water has been shown in Figure 6.

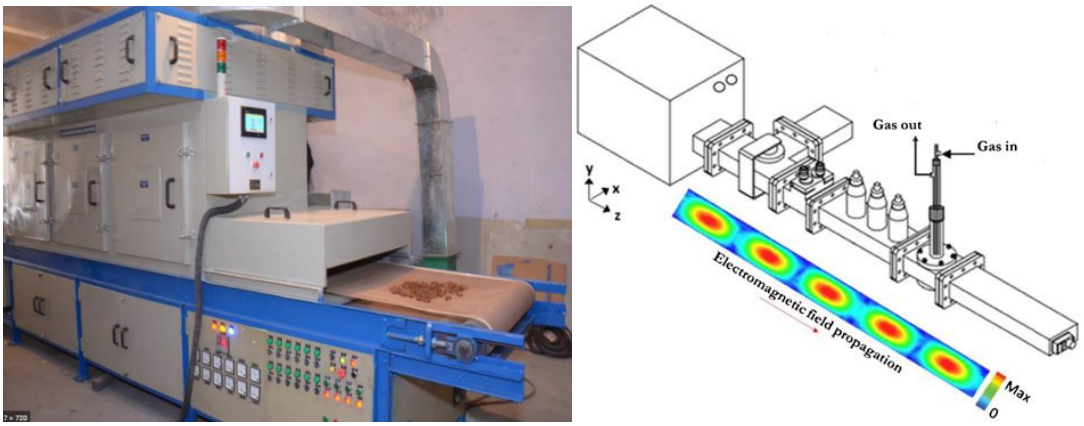

Figure 6. Illustration of microwave irradiation heating system [23]

2.2.2 Top-Down Synthesis of GQDs

The top-down method uses inexpensive and readily available bulk precursors from nano carbons, for exfoliation and decomposition in harsh environments to obtain GQDs using chemical, electrochemical, or physical methods. It is possible to cut bigger precursors such as graphite but, in most cases, it is ineffective because typically GQDs obtained from them have poor optical properties (which reduce the potential applications of GQDs), broad size distribution, and different particle shapes [21,24]. Compared to the bottom-up approach top-down method's advantages are mass production, simple synthetic routes, and cheap raw materials while the disadvantages are the requirement of multiple steps comprising of strong oxidizing agents, high temperatures, and concentrated acids. In addition, controlling the morphology and size distribution of GQDs is a challenging issue in the top-down approach because of the non-selective chemical cutting procedure.

2.2.2.1 Thermal Heating Process

Tian et al. (2018) mentioned that the most used method in the top-down approach is the hydrothermal method [25]. The hydrothermal process is preferred because the method is a green, environmentally friendly, low-cost, and nontoxic approach for GQDs synthesis using inexpensive bulk precursors such as reduced graphene oxide (RGO) sheets or graphene oxide (GO) sheets [21]. But depending on the chemicals that are used in the conventional process it can become very oxidizing, toxic to the environment, and could easily corrode the equipment while yielding around 5-20% of GQDs [25]. On the other hand, the solvothermal process is not considered as environmentally friendly and nontoxic approach as the hydrothermal process to obtain GQDs because of the organic solvents that are used such as dimethylformamide (DMF), benzene, or dimethyl sulfoxide (DMSO) which can yield as much as 45-50% of GQDs [26]. Shoujun et al. (2011) mentioned that the solvent's physicochemical nature will impact directly the morphology and size of the final product by adding epoxy groups on the carbon lattice which results in the size reduction of the bulk precursor to GQDs with the size at average 3.6-9.6 nm [14].

2.2.2.2 Electrochemical Exfoliation Process

Electrochemical exfoliation is the simple one-step method that can cut electrochemically different bulk precursors such as graphite rods, chemical vapor deposition (CVD)-grown graphene, (RGO/GO) films, carbon nanotubes/fibers, carbon black, soot, activated carbon, coal, and many more which always results in a high yield of GQDs that are at average size 3-5 nm [21,25,27]. There, as a result of anodic oxidation, water is transformed into $\bullet$OH and $\bullet$O radicals that cause corrosion of bulk precursor. In other words, these radicals initiate at the edge sites electrochemical scissoring which accelerates the forming of GQDs from defect sites. This method is so-called green because it does not use any strong (acids/bases) to accelerate exfoliation which will not corrode process equipment, but it has problems such as the impossibility of large-scale production and functionalization of GQDs to enrich the performance of the GQDs [28].

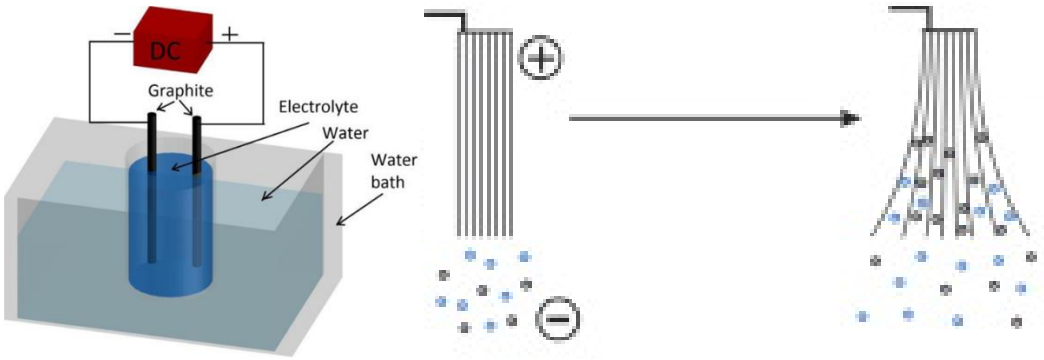

Figure 7. Illustration of electrochemical exfoliation process [28]

2.2.2.3 Acid Etching

GQDs can also be produced via acid etching which use strong acids such as HNO_3 to cut different bulk precursor through corrosion in the same way as in electrochemical exfoliation. The difference is that instead of only •OH and •O radicals there are present different negatively charged oxygenated groups [25]. Compared to electrochemical exfoliation this method can be used for large-scale production as well as to tune and enrich GQDs properties/performance. For example, by enhancing the defective sites and making their surfaces hydrophilic. However, strong acids corrode the equipment, and the removal of oxidizing agents is a great challenge [21].

2.2.2.4 Microwave Irradiation

This method is a combination of the advantages of microwave irradiation and acidic exfoliation which will as the result make a rapid and stable environment for the reaction. In other words, carbon bonds are agitated by microwave irradiation which not only makes heat control of the solution easier and faster (because only bonds are affected/heated while conventional process heat container and solution), but it also assists acids in exfoliation of raw material resulting in shorter reaction time with high yields of GQDs [21,25].

2.2.2.5 Ultrasonication Exfoliation

Another simple method is the ultrasonication exfoliation process. This method is non-corrosive, environmentally friendly, and a cost-effective method to produce GQDs [29]. It uses simple mechanical force to produce low- and high-pressure waves in the liquid to generate vacuum bubbles that will grow in size and undergo violent collapse generating momentarily high temperature and pressure. These cause deagglomeration, strong hydrodynamic shear forces, and high-speed impinging liquid jets which are capable to turn bulk precursors into GQDs. On another hand, it is possible to use ultrasonic treatment under acidic conditions to oxidize bulk precursors into 3-5 nm GQDs but to produce uniform-sized GQDs multiple steps need to be used e.g., oxidizing precursors in an acidic solution while under microwave or solvothermal treatment which yields around 20% of GQDs [21,29].

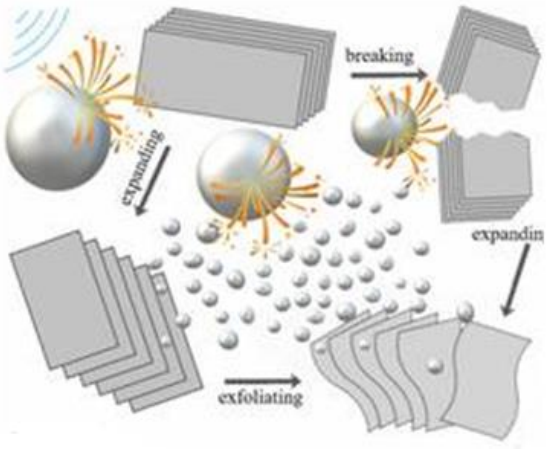

Figure 8. Illustration of ultrasonication facilitation [30]

2.2.2.6 Electron Beam-Lithography Process

In the lithography process, GQDs are carved from large graphene flakes that are placed onto SiO_2/silicon wafer by cutting electron beams-irradiated graphite through hydrazine reduction under 100 °C. It is reported by Massabeau et al. 2018 that using E-beam lithography is possible to draw wanted shapes on the surface of graphene flakes that are sandwiched by an electron-sensitive film such as hexagonal Boron Nitride crystal layers which is transferred onto silicon substrate followed by electron/ion beam that enables selective removal of non-exposed or exposed regions of the electron-sensitive film by

immersing it in a solvent [31]. The average size of GQDs obtained from the process is 3-50 nm because the resolution is limited in this process and the isolation of the graphene flakes is meticulous such as optical identification of the flake's layers. In addition, the quality depends on several factors such as surface cleanliness, chemical bond splitting method of the graphite as well as wafer layer thickness.

2.2.2.7 Chemical Exfoliation

Chemical exfoliation is the process where, as the name suggests, under acidic conditions chemicals exfoliate GQDs from the graphitic structure by oxidation reactions which are known as Hummer's method. Strong concentrated acids such as HNO_3 and H_2SO_4 are used to treat Carbon fibers (CFs) over 24 hours at high temperatures. It was discovered that average GQDs size is tuneable depending on the temperature in which the CFs were oxidized for example, at 80°C 1–4 nm GQDs while at 120°C 7–11 nm GQDs can be obtained respectively, while their topographic heights wary from one to three graphene layers. This method works for CFs and CX-72 carbon black. Also, it is possible to first dissect graphite into graphene nano blocks by fragmentation approaches such as diamond edge-induced technique or "nanotomy" technique after using chemical exfoliation to produce GQDs [21,25].

2.3 Purification Process

Effective and economical purification of GQDs from unreacted components or other impurities, that have been formed along the synthesis or are remnants of the catalysts, is equally as important as an effective synthesis method. The reason why purification is important is that in many applications (for example, such as medicine or wastewater treatment) impurities can lead to side reactions which in the case of water treatment will bring ineffective pollution removal and economical loss or in the medical field it can lead in the worst case to death. That is why this chapter will be discussed different purification methods that utilize the difference in chemical and physical properties of GQDs and impurities to separate them.

2.3.1 Size-Based Separation

Size-based selective separation or isolation, such as size exclusion chromatography (SEC), is widely used for the purification of nanoparticles (NPs) which are in size up to 100 nm. The principle of chromatographic methods is to pass the synthesized NP solution through a porous stationary phase (SP). Particles that are smaller than the effective molecular weight cut-off (MWCO) will be adsorbed on porous SP. This method enables to do continuous purification through adsorption and desorption cycles. Compared to other methods chromatography is a scalable and much simpler method because there is a wide variety of different SPs and elution solutions making it possible to take advantage of synthesized GQDs characteristics and easier to separate [32].

Other methods to selectively separate GQDs by utilizing their size are filtration and centrifugation. The filtration method is based on the molecular size of GQDs and the cut-off of the porous filter membrane. The molecules that have a smaller size than the cut-off membrane can easily pass through it while bigger ones will be retained. It can be used to separate GQDs from bigger particles or smaller particles depending on which synthesis approach was GQDs synthesized. The negative side of this method is that it often leads to losses by particles sticking to the filter [33]. On another hand, centrifugation utilizes mass (such as colloids), density, or polarity difference of solution to separate GQDs from impurities usually when a synthesis method is a bottom-top approach [34,35]. Thus, if GQDs are big enough then synthesized GQDs solution can be put through ultracentrifugation without any pre-treatment while if GQDs are not big enough then pre-treatment will be needed before putting it through ultracentrifugation. Pre-treatment can be done by adding an organic or an inorganic medium which will attach itself selectively to either GQDs or impurities making separation easier. For example, there are several reports where CA was successfully removed from the solution by making it into a colloid through centrifugation (aluminum hydroxide was used as a core for the colloid) or by using a magnet (iron (II or III) oxide was used as a core for colloid) [36,37]. The negative side of this method is that it needs repeated centrifugation to get a good yield.

2.3.2 Electrophoresis

Electrophoresis is the method where electrical or magnetic properties of GQDs are utilized for a continuous separation process. In this process, as-synthesized GQDs solution flows through the electric field (differently charged plates), or electric and magnetic field (electricity goes through the wire). As a result, when GQDs, that have a charge which can be ionic +/- charge, or many weak dipole-dipole charges, are exposed to an electric field (or at the same time to a magnetic field as well) they will be separated from impurities. Of course, it all depends on the edge of GQDs (charge) and their size. In some cases when GQDs are large that it is hard to move or do not have charge then impurities can be separated from unmoving GQDs. The conventional electrophoresis process has one inlet, a passage where only a magnetic field is applied, and two outlets where one is for separated GQDs, and another is for impurities. On another hand, in the new method porous electrodes are integrated into the process while an electric field is applied between them. This new method collects GQDs on the electrodes while impurities pass through the porous electrodes which are more effective than a process without electrodes [38–40].

2.3.3 Extraction

Extraction is an alternative method for the purification of GQDs. It is based on the difference in solubility between GQDs and contaminants in solvents with different polarities [20]. In general, extraction is gentler than precipitation/redispersion, because NPs remain in their original phase, which results in a reduced probability of their irreversible aggregation. However, small-molecule impurities can be trapped in the precipitated GQDs matrix or strongly adsorbed onto the GQDs surface and, hence, numerous cycles of extraction are required for effective elimination of the lowest-molecular-weight contaminants. As in the case of the precipitation/redispersion method, this results in the reduction of ligand density and degradation of colloidal stability and functional properties of the GQDs or their conjugates. Electrophoretic purification methods apply to poly (ethylene glycol) (PEG)-coated, lipid-micelle-encapsulated [21], and protein-conjugated GQDs [22]. However, these methods are poorly scalable and, in general, also disrupt the colloidal stability of NCs.

3 Experimental Part

To find the most effective way to synthesize GQDs of the wanted size it is important to know the optimal environment and composition. That is why the next chapters will be described the materials, experimental, and analytical methods used in this thesis.

3.1 Materials and Characterization

Analytical grade reagents were used in this study without further purification and purchased from Sigma-Aldrich and VWR Chemicals. The Citric acid (99.5%), and D(+)-glucose anhydrous were used as carbonization precursors while Sodium hydroxide (99%) was used as a catalyst.

Characterization of synthesized GQDs was performed using Agilent Technologies Cary Series UV-Vis-NIR spectrophotometer, Agilent Technologies Cary Eclipse Fluorescence Spectrophotometer, and (TEM, HT7700) Transmission Electron Microscopy (TEM). Firstly, after seeing that every synthesized solution/mixture did emit PL, under EL Series UV lamp that used 8 Watt powered longwave filtered BLB 365 nm lamp, all mixtures/solutions were diluted with pure water until the concentration of initial CA (before synthesis) was 0.01M. After what solutions were filtered using a 45 μm and 20 μm syringe filter to remove big particles and were put through a UV-Vis-NIR spectrophotometer which parameters were set to have an excitation wavelength range from 200 nm to 600 nm and pure water as a background. These samples were further analyzed with the use of a Cary Eclipse Fluorescence Spectrophotometer which parameters were set to have excitation wavelength change every measurement round for 5 nm starting from 200 nm and finishing at 550 nm while the measurement of excitation intensity was set to be from 250 nm to 700 nm. Finally, the samples that showed the best results in the previously mentioned characterizations were diluted in pure water until 0.1 m-% for the TEM analysis (at an accelerating voltage of 100 kV under HR lens mode).

3.2 Synthesis of GQDs

I decided to use the hydrothermal method and microwave irradiation to synthesize GQDs using the bottom-up approach. These two methods are known as the greenest methods if used precursors/chemicals are bio-based such as CA or D(+)-glucose anhydrous.

3.2.1 Hydrothermal Methods

I performed two initial experiments to investigate the workability of the precursor and alkaline catalyst which is NaOH on the GQDs formation. The first synthesis was done using the hydrothermal method as described in the literature [41] while the second one was performed in the same way but without using NaOH. It was also decided based on Figure 9 that Teflon-autoclave will not be filled more than 50% of the total volume because of the possible pressure generation inside and other safety reasons while used temperatures in the synthesis were below 200 °C.

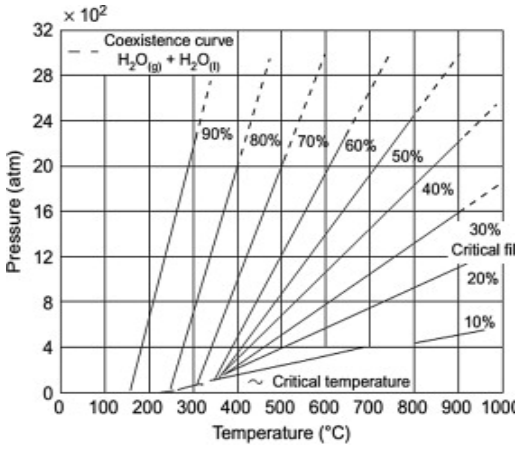

Figure 9. Pressure generation inside closed vessel depending on the temperature [42]

Based on the literature study of GQDs formation was performed at 180 °C temperatures for 5 hours. Firstly, the two solutions were prepared by mixing 3.2 g of CA in 80 ml of pure water and the pH of one solution of the two was adjusted to 10 by using 0.1 M NaOH. The mixtures were stirred for 30 min at room temperature followed by 1-hour ultrasonication. After that 45 ml of solution was poured into a 90 ml Teflon autoclave followed by moving

them inside the oven to start the heating process. In the result, one solution with poor PL and one without were obtained proving the workability of the CA as the precursor.

3.2.1.1 Effect of Process Temperature on the GQDs Synthesis

After confirming that CA can be used as the precursor for GQDs synthesis the next step was to study how to process temperature can affect the GQDs synthesis when reaction time is held constant. Temperature dependence studies have been performed with CA, pure water, and NaOH in the composition (Table 3).

Table 3. The components and the amount of Sam1 solution

Component	Amount (g)	(m-%)
Citric Acid	177.86	34.6
Pure Water	305	59.4
Sodium Hydroxide	30.65	6

To investigate the effect of temperature on the formation of GQDs, the carbonization degree of CA was studied at different temperatures for a constant duration. These synthesizes were performed using the same methods that have been described in the previous chapter the only difference was in the composition of the components that were used. I prepared the solution (labeled as Sam1) by adding 177.86 g of CA and 30.65 g of powdered NaOH in the presence of 305 ml of pure water.

Figure 10. Filled Teflon autoclave placed inside the Termaks 8000 oven

The experiments were performed using the same Sam1 solution in four different temperatures which were 170, 180, 190, or 200 °C for 5 hours (Table 4), and then the solution was left to cool inside the oven until room temperature. Finally, synthesized GQDs were diluted in pure water and stored in a fridge.

Table 4. Synthesis in different temperatures for 5 hours

Name	Temperature (°C)	Time (h)
Sam1-GQD-170-5h	170	5
Sam1-GQD-180-5h	180	5
Sam1-GQD-190-5h	190	5
Sam1-GQD-200-5h	200	5

3.2.1.2 Reaction Time Efficiency in Different Process Temperatures on the Synthesis

To investigate the efficiency of reaction time in different temperatures on the formation of GQDs, the experiments were carried out at three different temperatures for different durations of time. The temperatures used in synthesis were 180°C, 190°C, and 200°C while each temperature was performed in four experiments for different duration of time which were 5 hours, 7.5 hours, 10 hours, and 12.5 hours for 180°C, and 2.5 hours, 5 hours, 7.5

hours, and 10 hours for 190°C and 200°C. These synthesizes were performed using the same solution “Sam 1” and methods that have been described in the previous chapter the only difference was in the reaction time that was set. Table 5 are summarised the names and conditions of the experiments.

Table 5. Synthesizes in 3 different temperatures for different reaction time

Name	Temperature (°C)	Time (h)
Sam1- GQD-180-5h	180	5
Sam1- GQD-180-7.5h	180	7.5
Sam1- GQD-180-10h	180	10
Sam1- GQD-180-12.5h	180	12.5
Sam1- GQD-190-2.5h	190	2.5
Sam1- GQD-190-5h	190	5
Sam1- GQD-190-7.5h	190	7.5
Sam1- GQD-190-10h	190	10
Sam1- GQD-200-2.5h	200	2.5
Sam1- GQD-200-5h	200	5
Sam1- GQD-200-7.5h	200	7.5
Sam1- GQD-200-10h	200	10

3.2.1.3 Influence of Mass Composition on the GQDs Synthesis

To investigate the influence of m-% of the composition of the main components (CA, NaOH, and ultra-pure water) on the GQDs formation, the experiments were carried out at 180 °C temperature for 5 hours. Ternary/Gibbs Diagram was used (Figure 11) to choose the composition of the components. The dots on the diagram represent the tested compositions of the compounds.

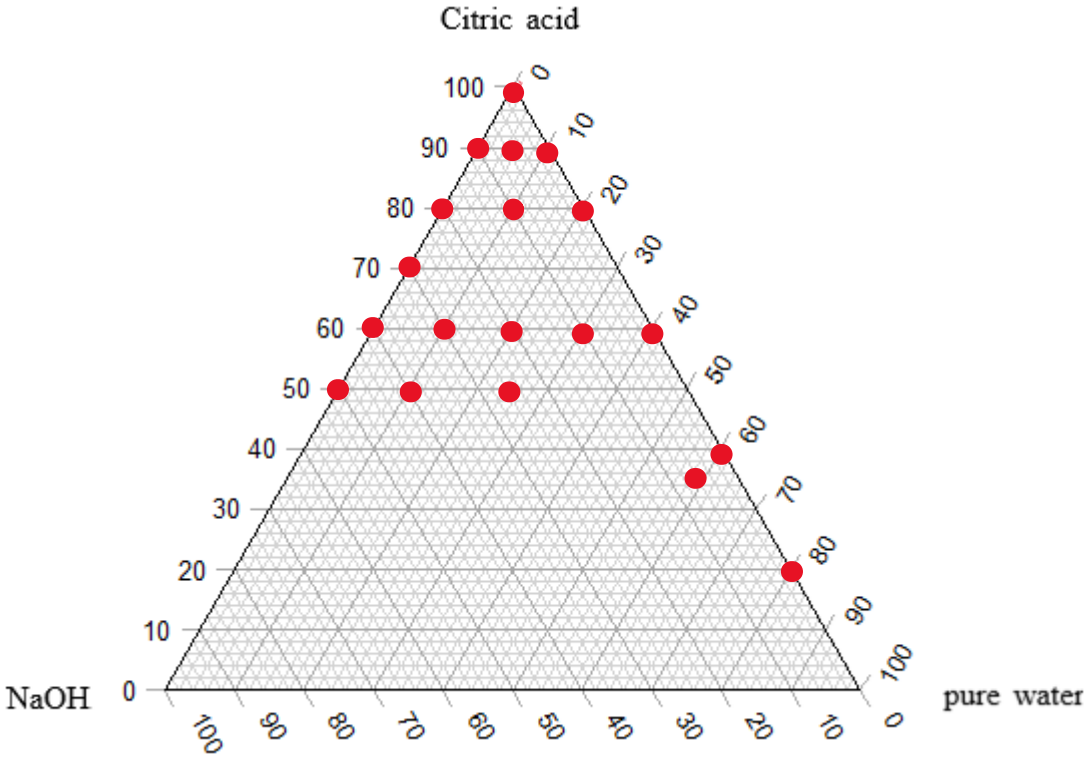

Figure 11. Ternary/Gibbs Diagram using NaOH, pure water, and Citric acid to find the best composition [25]

The samples were prepared in the same way as was described in chapter 3.2.1.1 except for the m-% of the components (Table 6) and the total mass of the samples which was 40 grams.

Table 6. Component ratios for Ternary diagram test

Test number	Citric acid (m-%)	Water (m-%)	NaOH (m-%)
Sam1-GQD-180-5h	34.6	59.4	6
Ternary 1	90	10	0
Ternary 2	80	20	0
Ternary 3	60	40	0
Ternary 4	40	60	0
Ternary 5	20	80	0
Ternary 6	100	0	0
Ternary 7	90	0	10
Ternary 8	80	0	20
Ternary 9	70	0	30
Ternary 10	60	0	40
Ternary 11	50	0	50
Ternary 12	90	5	5
Ternary 13	80	10	10
Ternary 14	60	10	30
Ternary 15	60	20	20
Ternary 16	60	30	10
Ternary 17	50	10	40
Ternary 18	50	25	25

3.2.1.4 Effect of Precursors on the GQDs Synthesis

To investigate the effectiveness of different precursors on the formation of GQDs, the experiments were carried out using D(+)-glucose anhydrous as a second precursor at a temperature of 180 °C for 5 hours which were found to be optimal for GQDs synthesis when CA was used as precursor. The sample was prepared in the same way as it was described in chapter 3.2.1.1 except for the use of different precursor and volume (40 ml). Table 7 is shown the conditions of the process and used composition.

Table 7. Mass composition and the synthesis conditions

Test name	Precursor	Glucose/NaOH/water (m-%)	Temperature (°C)	Time (h)
Glucose-180C-5h	glucose	35% / 6% / 59%	180	5

3.3 Microwave-Assisted Synthesis

Another interest of this study is the microwave irradiation process which is said to be more effective and "greener" than the conventional thermal process. It is a known fact that microwave irradiation affects molecular structure i.e., bonds directly which as result produces a reaction, as mentioned in the 2.2.1.2 chapter. To check the effectiveness of microwave irradiation on GQDs synthesis and its impact on GQDs properties it was decided to carry out experiments using a commercial microwave oven under 800W in the same composition as in Ternary 2 and Ternary 13. The samples were prepared in the same way as was described in chapter 3.2.1.3 except instead of putting samples inside the oven, they were put in a microwave oven for 1 minute (Table 8).

Table 8. Conditions of microwave irradiation synthesis

Name	Watt (W)	Irradiation duration (min)
GQDs-800W-Ternary 2	800	0,9
GQDs-800W-Ternary 13	800	0,9

4 Results and Discussion

This chapter will be discussed and described the results of the performed experiments and analyses.

4.1.1 Usability of Precursors

The initial experiment was performed as described in the literature [41] while the second experiment was performed in the same way but without using NaOH. In those two experiments were tested if CA is usable as the precursor and if NaOH can be used as the catalyst. From the synthesized products could be seen that synthesis performed as described in the literature had poor PL properties. On the other hand, the synthesis performed without using NaOH could not produce PL that could be seen by the naked eye (Figure 12).

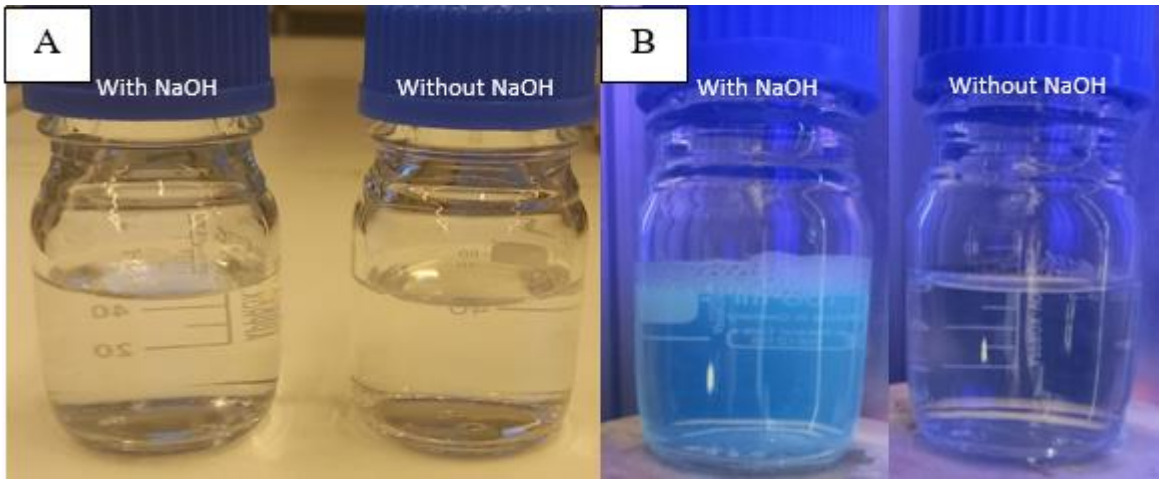

Figure 12. Synthesized products in daylight (A) and their PL under irradiation of (365nm) longwave filtered BLB lamp (B)

Based on these results it can be concluded that the reaction using an alkaline catalyst can be divided into two stages, in the first stage depending on pH carboxyl groups of CA can lose a hydrogen ion and become negatively charged oxygen radicals making precursors more reactive (Figure 13). But in the second stage, if the temperature is enough, oxygen radicals will react with other molecules resulting in the formation of GQDs while at the same time weak interactions with Na^+ further accelerated GQDs formation. On the other hand, poor PL

is the result of big amounts of used pure water as well as water that came from 0.1M NaOH solution used in pH adjustment. This made it harder for the precursor to come close to each other which slowed the carbonization process resulting in less effective synthesis.

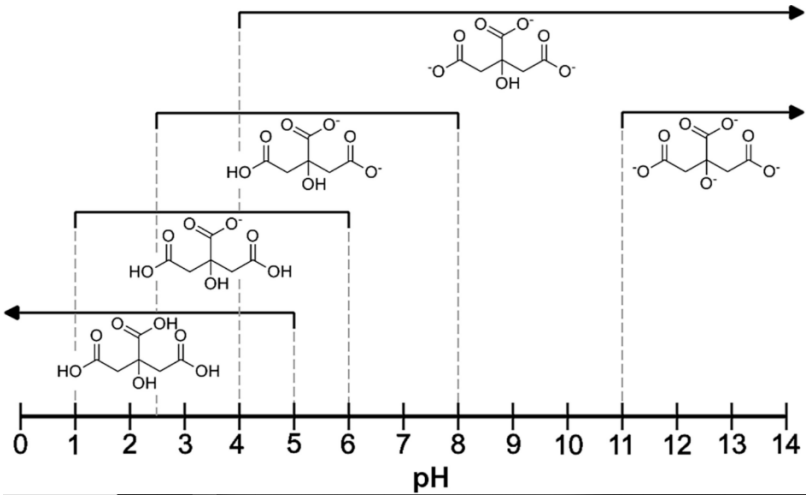

Figure 13. How pH affects CA precursor reactivity [43]

Sang et al. (2020) said that other alkalis and salts have similar catalysis effects on the carbonization process [44]. The reason behind this is due to weak interactions between ions of the alkalis and salts with precursors which is the reaction between precursor's hydroxyl groups (-OH) and alkalis/salts. But even if it is said that salts have a similar effect as alkalis it does not mean that conversion of the precursor to GQDs will be the same! The reason behind this is the reactivity of precursors in different pH's. Precursors will become more reactive in higher pH values the more hydroxyl groups the precursor has or if it is acidic because in the alkaline environment it starts to lose hydrogen ions (H^+) becoming negatively charged. On another note, if the solution has an alkaline compound that is made of sulfur, fluorine, phosphor, or nitrogen then it is possible to functionalize GQDs and change the excited state which the result will produce different colored PL emissions.

4.1.2 Results of Process Temperature Effect on the GQDs Synthesis

It is a known fact that hydrothermal carbonization will start only when the temperature is above the melting point of the organic precursor. In this study, CA was used and its melting point is 153°C. That is why tests were performed at temperatures of 170°C and higher because 160°C in my option is not sufficient for effective synthesis. After carrying out synthesizes described in chapter 3.2.1.1 the products were put under UV lamp irradiation (Figure 14 (B-C)) to confirm that they emit PL.

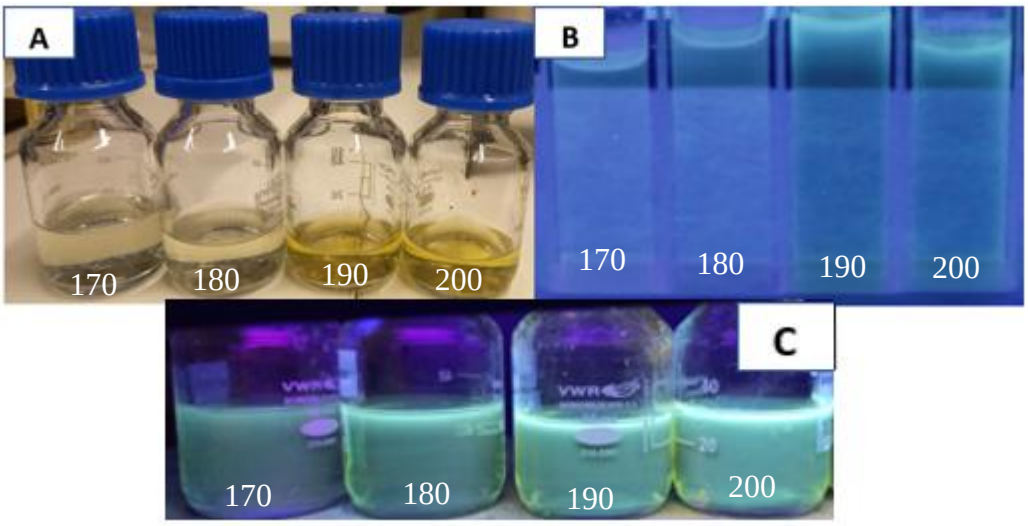

Figure 14. Synthesized products in daylight (A) and their PL under irradiation of (365nm) longwave filtered BLB lamp (B and C) starting from left to right Sam1-GQD-170 -5h, Sam1-GQD-180-5h, Sam1-GQD-190-5h, and Sam1-GQD-200-5h

As can be seen in Figure 14, there is a clear change in color (A) and intensity (B and C) of the synthesized products that were performed at 180°C and 190°C temperatures. It is known that an increase in temperature typically accelerates reaction because it will raise the average kinetic energy of the reactant molecules. Therefore, a greater proportion of molecules will have the minimum energy necessary for an effective collision, and the time needed to get the same results will be decreased. These optical properties were further studied by UV-Vis-NIR spectrophotometer (Figure 15), and fluorescence spectroscopy (Figure 16) to explain this change in color and PL intensity.

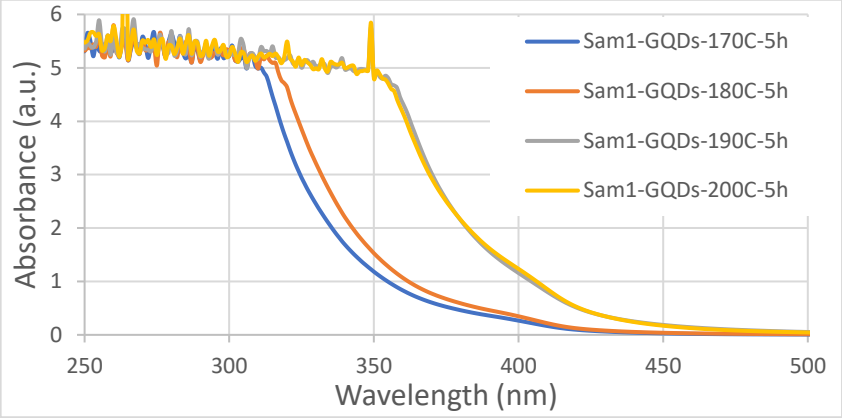

Figure 15. The absorption spectra of the experiments performed at different temperatures for 5 hours

Yang et. al. (2015) mentioned that the aromatic structure of GQDs shows a typical π-π^* transition absorption peak around 250 nm, a n-π^* transition absorption peak around 340 nm, and a long tail extending into the visible range [45]. Figure 16 shows the same behavior as what was described by Yang et. al. (2015). The reason behind the absorption peak at a wavelength around 250 nm is the sp^2 domains of the structure which are C=C bonds and possibly unreacted C=O of the carboxyl group while the absorption peak at a wavelength around 340 nm and the long tile extending into the visible range is due to abundant carboxylic or hydroxylic groups which change excited state and thus needed excitation wavelength.

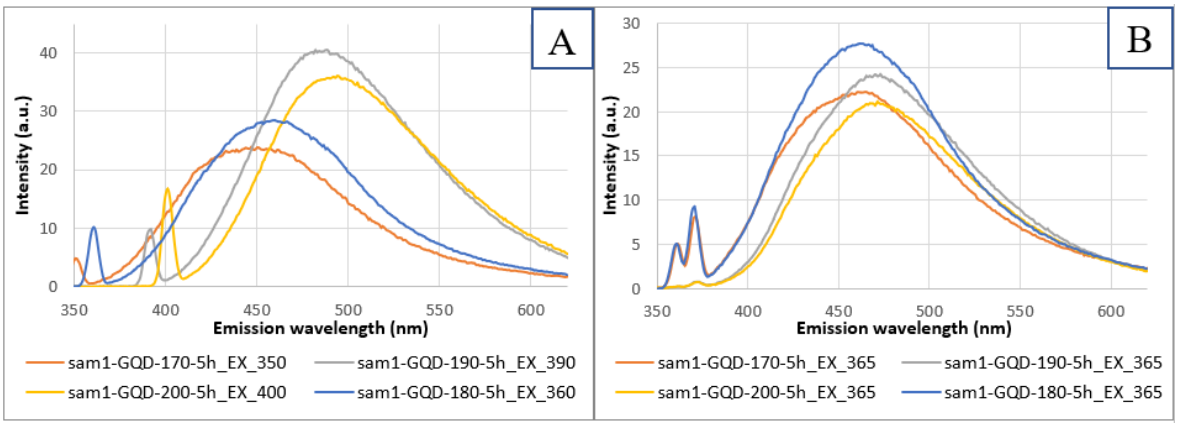

Figure 16. (A) PL spectrum of strongest intensity in respective synthesized products and (B) PL spectrum at the specific excitation wavelength (365 nm)

Figure 16 (A) presents the PL spectrum plot, where was used excitation wavelengths that give the strongest emission intensity in each synthesized product. There can be seen how temperature affects excitation wavelength growth as well as how the strongest intensity

giving emission wavelength shifts to the right which is seen as the excitation wavelength, needed for PL, and emission wavelength growth. On the other hand, Figure 16 (B) used an excitation wavelength of 360 nm to see how the transition state is affected by the reaction temperature. It is seen that the higher the temperature the longer wavelength is emitted even if the excitation wavelength is held constant. This difference between absorption and emission wavelength, which is from 90 nm to 115 nm, indicates that it can be due to the abundant carboxylic or hydroxylic groups, the different surface states of GQDs, by-products that have PL properties, or GQDs particle sizes.

These observations indicate that increase in the temperature from 170°C to 200°C affects carbonization kinetics in form of shift/change in the absorption wavelengths between 320-450 nm and their emission wavelengths. Proving that when the temperature is raised, over the precursor's melting point, the solid mixture will be liquidized making it condensed while vapor pressure, which grows with the increase of temperature, will make the liquidized solution more condensed accelerating the reaction. The most significant change is moving from 180°C to 190°C indicating that this 10°C difference makes CA react faster and conversion of CA is higher.

To find out if the increase in temperature will produce more GQDs TEM images were performed (Figure 17). The GQDs synthesized at 180°C for 5 hours using the "Sam1" solution clearly shows the existence of GQDs and their morphology. Contrarily, products synthesized at temperatures 190°C and higher did not show GQDs in TEM images. More precisely, products synthesized at the temperature of 190°C showed the presence of nanofibers that had GQDs or something that resembled GQDs attached on their surface while products synthesized at the temperature of 200°C showed agglomerated clusters that resembled that of carbon quantum dots. This observation indicates that at temperatures higher than 180°C CA react faster and the conversion of CA is higher but synthesis goes out of the control and does not produce GQDs. So, it was concluded that the optimal synthesis temperature is 180°C, and produced average diameter of GQDs using "Sam1" composition is 4.5±1.5 nm (Figure 18).

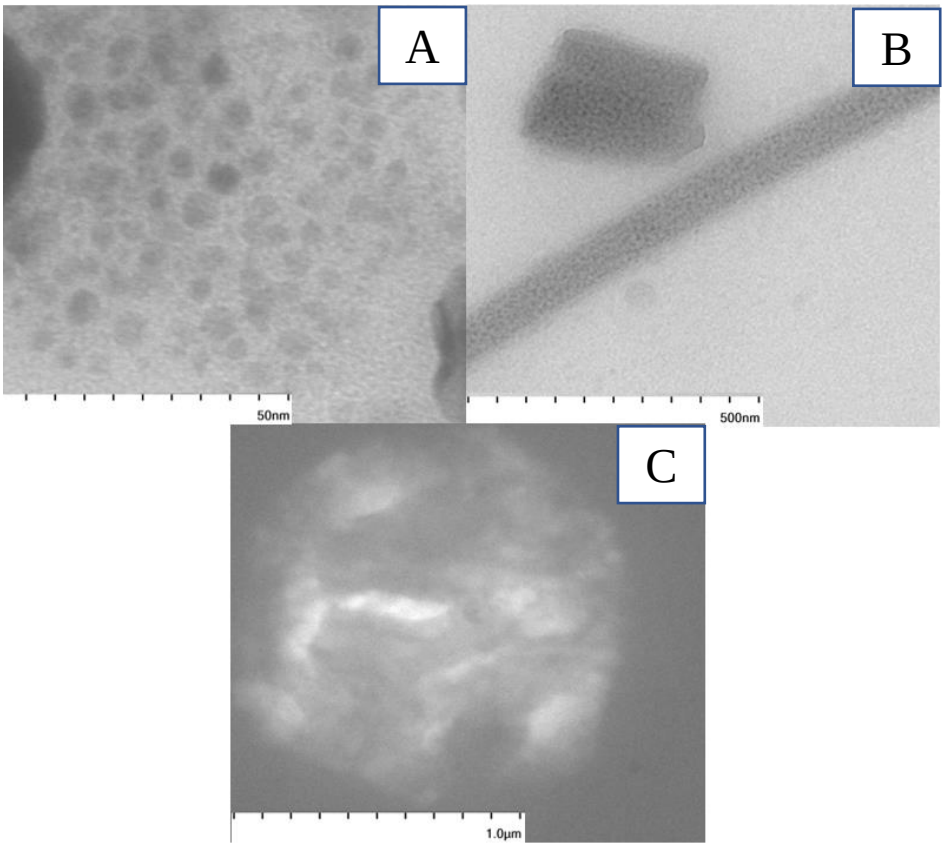

Figure 17. TEM images of products synthesized for 5 hours at A) 180°C, B) 190°C, and C) 200°C

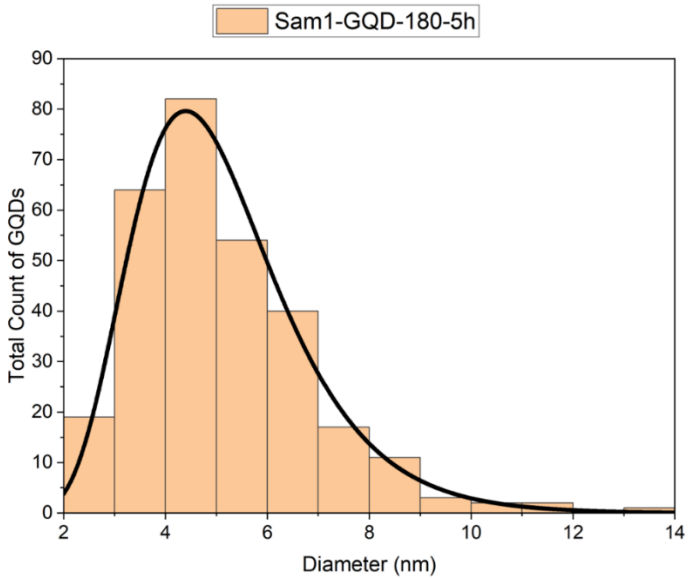

Figure 18. Histogram of all GQDs found in Sam1-GQDs-180C-5h synthesis product

4.1.3 Results of Reaction Time Efficiency in Different Process Temperatures

The reason to perform the test in three different temperatures and not in one was to see not only how reaction time affects carbonization of CA (i.e., GQDs size and amount) but also to see how fast it will be, depending on the used temperature. In the case of 180°C, the extra 2.5 hours were used every time to counteract the effect of the temperature. The reason why experiments did not include a temperature of 170°C is that in my opinion, the said temperature would not be effective enough compared to a temperature of 180°C. After carrying out synthesizes described in chapter 3.2.1.2 there could be seen that except for Sam1-GQD-180-5h every other synthesis product had orange/light brown color and they had the same color of fluorescence to the naked eye under UV lamp irradiation at the excitation wavelength of 365 nm (Figure 19).

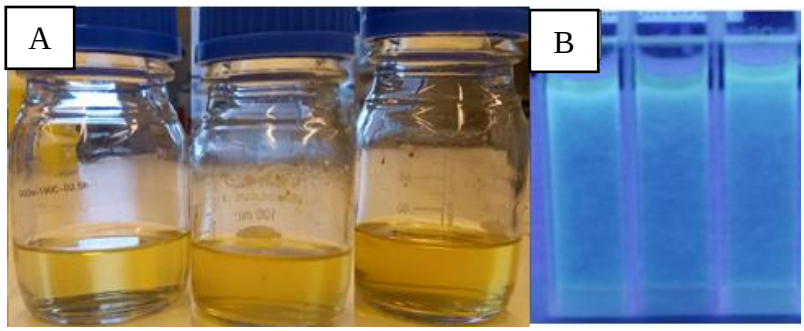

Figure 19. Synthesis results (A) and their PL (B) starting from left to right Sam1-GQD-180-12.5h, Sam1-GQD-190-10h, and Sam1-GQD-200-10h

The optical properties of these synthesis products were further studied by UV-Vis-NIR spectrophotometer (Figure 20), and fluorescence spectroscopy (Figure 21).

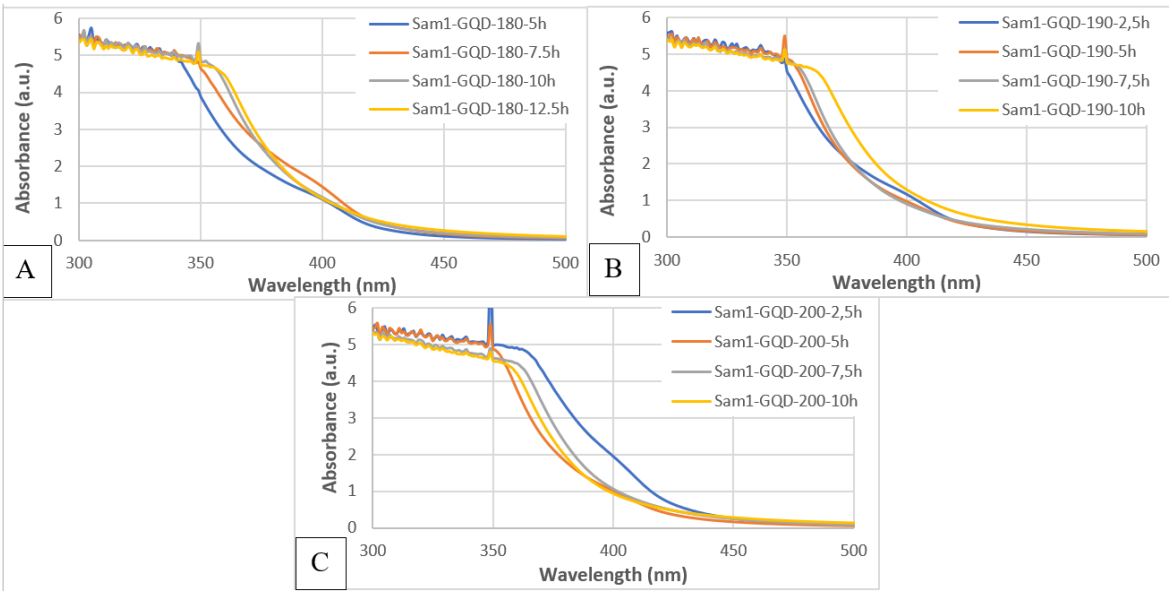

Figure 20. The absorption spectra of the experiments performed at (A) 180°C, (B) 190°C, and (C) 200°C temperatures

As can be seen from Figure 20 (A) and (B), the temperature has a strong effect on shortening reaction time if absorption spectra of synthesized at temperatures of 180°C for 5 hours and 190°C for 2.5 hours are compared. Contrary to expectations, synthesis experiments that were performed at 200°C show that their absorption spectra do not follow a trend as experiments carried out at temperatures of 180°C and 190°C e.g., longer reacted showed stronger absorption spectra than those that had lower reaction time. Based on this observation could already be said that synthesis at 200°C temperature does not produce GQDs.

After the TEM analysis (Figure 17) I compared them with the plots in Figure 20. Observed patterns of absorption spectra synthesized at 200°C temperature indicates that there is no GQDs present. While absorption spectra of synthesizes carried at 180°C and 190°C temperatures indicate the presence of GQDs.

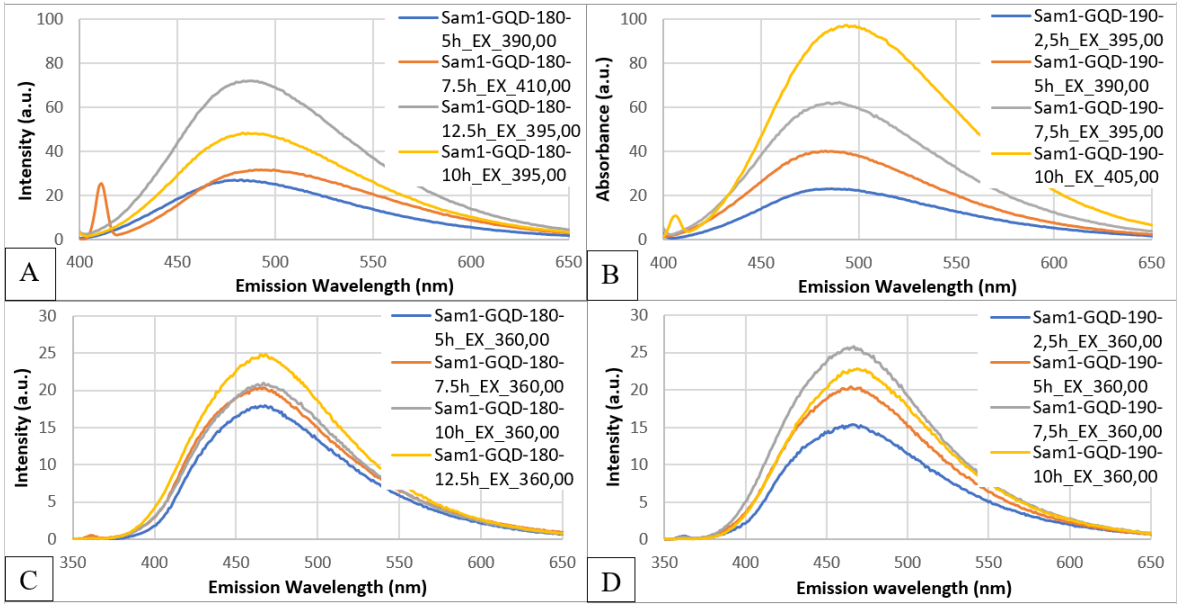

Figure 21. (A) and (B) the PL spectrum of the strongest intensity of the experiment carried out at 180°C and 190°C respectively and (C) and (D) the PL spectrum at the specific excitation wavelength (360 nm) of the experiment carried out at 180°C and 190°C respectively

In Figure 21 (A) and (B) are PL spectrum plots, where was used excitation wavelength that gives the strongest emission intensity synthesized using temperatures of 180°C and 190°C respectively for different duration of time. From these two plots can be seen same behavior as was observed in the previous chapter (Figure 16 (A)) e.g., the excitation wavelength needed for the strongest PL intensity and strongest intensity giving emission wavelength growth/shift to the longer wavelength the longer it reacts. Figure 21 (C) and (D) used an excitation wavelength of 360 nm to plot the PL spectrum of the experiment carried out at 180°C and 190°C respectively. These plots have the same behavior as discussed in the previous chapter (Figure 16 (B)) e.g., the transition state was affected by the reaction time but compared to the different temperatures the difference is not big. This indicates that particle size and surface state of GQDs are the same and only the amount is different.

Another interesting observation that was made is brown aggregation inside of the few experiments which did not want to dissolve into solution even after 2 hours of sonication and mixing. In Figure 22 can be seen Sam1- GQD-190-10h, and Sam1- GQD-200-7.5h experiments with the beforementioned brown aggregation.

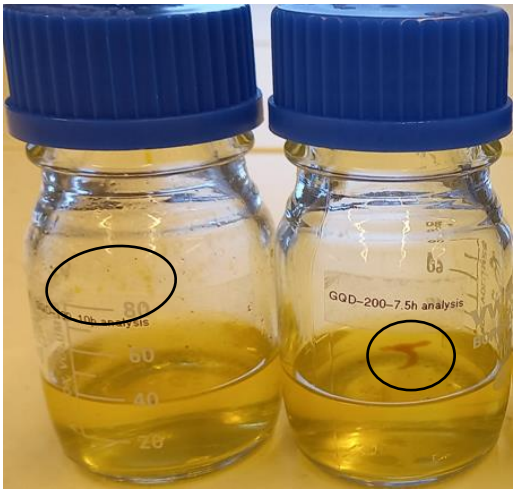

Figure 22. Synthesis results with brown aggregation starting from left to right Sam1- GQD-190-10h, and Sam1- GQD-200-7.5h

This phenomenon was only observed in the experiments that were synthesized at temperatures of 190°C and 200°C. Based on previous results this aggregation is a by-product of the synthesis or agglomeration of GQDs in one cluster. Manikandan et al. 2019 also mentioned that aggregation is one of the problems of GQDs synthesis using a bottom-up approach [21]. It makes sense because in addition to by-products it also makes usable GQDs react with each other turning them into unneeded clusters. This statement made by Manikandan et al. 2019 also indicates that it is impossible to synthesize GQDs with the high conversion of precursor because agglomeration will take place reducing the amount of GQDs.

4.1.4 Ternary/Gibbs Results

I performed experiments in different mass fractions to find optimal composition where GQDs could be synthesized successfully/effectively in big quantities and with the minimum quantity of by-products and aggregations. Based on the results described in previous chapters it can be concluded that the optimal temperature to carry out synthesizes is 180°C as well as

optimal reaction time for the synthesizes is 5 hours. Thus, I decided to use these temperature and reaction time parameters to find an optimal composition. After carrying out synthesizes described in chapter 3.2.1.3 there could be seen that every synthesis product had different colors in visible light such as white, yellow, orange, red, and transparent as well as different PL under UV lamp irradiation (Figure 23).

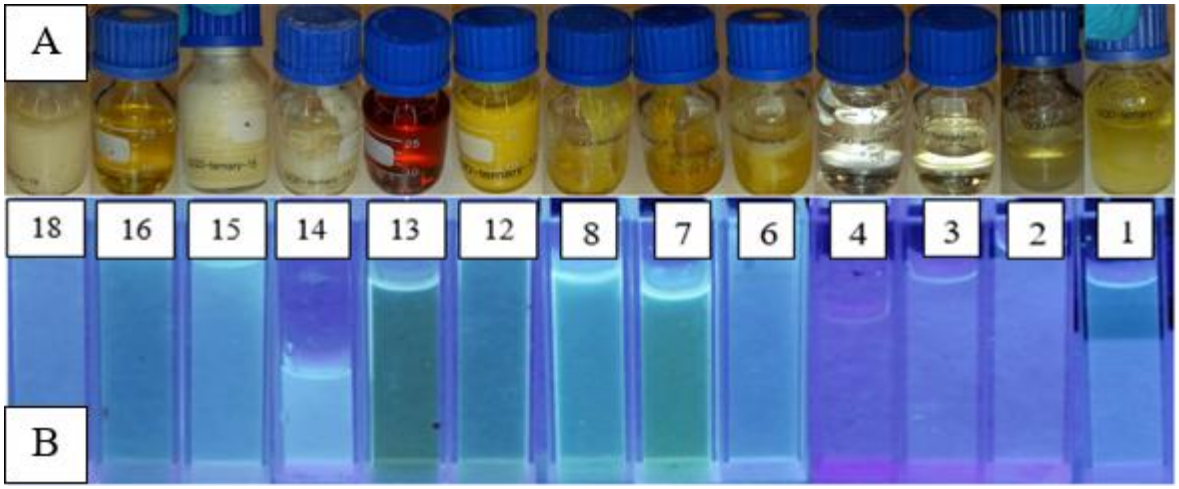

Figure 23. (A) Synthesis products under visible light and (B) their PL under UV-lamp irradiation (365 nm) starting from left as Ternary 18 (marked as 18) and ending on the right as Ternary 1 (marked as 1)

In Figure 23 can be seen how the presence of NaOH and water affect the product's color under visible light and their PL under UV-lamp irradiation which is connected to the conclusions discussed in chapter 4.1. It also was proved in the previous chapters that by-products and aggregations have absorption and PL spectrum that resembles that of GQDs. Because of these conclusions, the observed optical properties of these synthesized products were further studied in the following steps. Firstly, to see how composition affects the absorption spectrum I performed dilution of every sample until 0.01M concentration, so that even the smallest change could be seen, and performed UV-Vis-NIR spectrophotometer analysis (Figure 24). Using absorption spectra were chosen 7 samples to perform TEM analysis (Figure 26) to find out around what composition GQDs are produced.

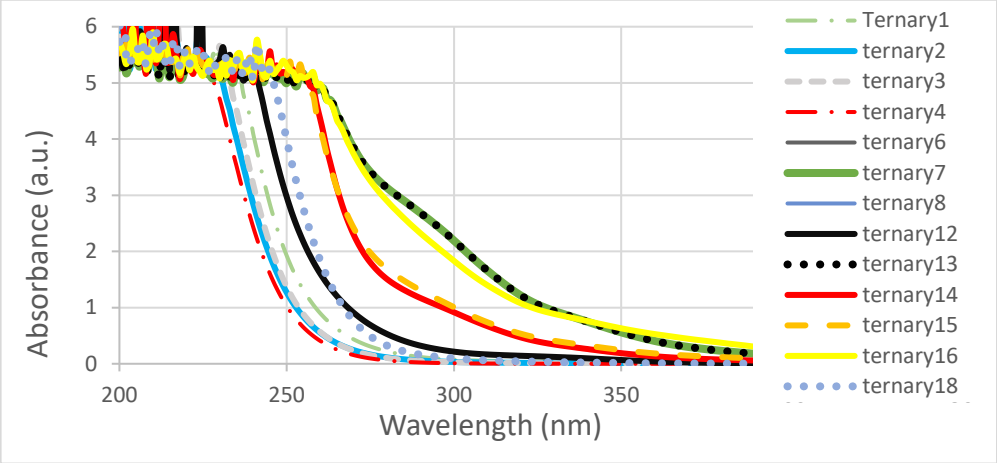

Figure 24. The Absorption spectra to the equally diluted Ternary experiments performed at 180°C for 5 hours

As could be seen from Figure 24, the dilution of samples helped to separate them to see how Pure water, CA, and NaOH, in different mass fractions, affect the absorption spectrum. From these 13 successfully synthesized products the chosen 7 samples were Ternary 2, 6, 7, 8, 13, 14, and 16. I compared the Ternary spectrum with the Sam1-GQD-180-5h which showed the presence of GQDs in TEM images (Figure 25 (A)) and chose 7 samples (Figure 25 (B)). After that TEM analysis was done (Figure 26).

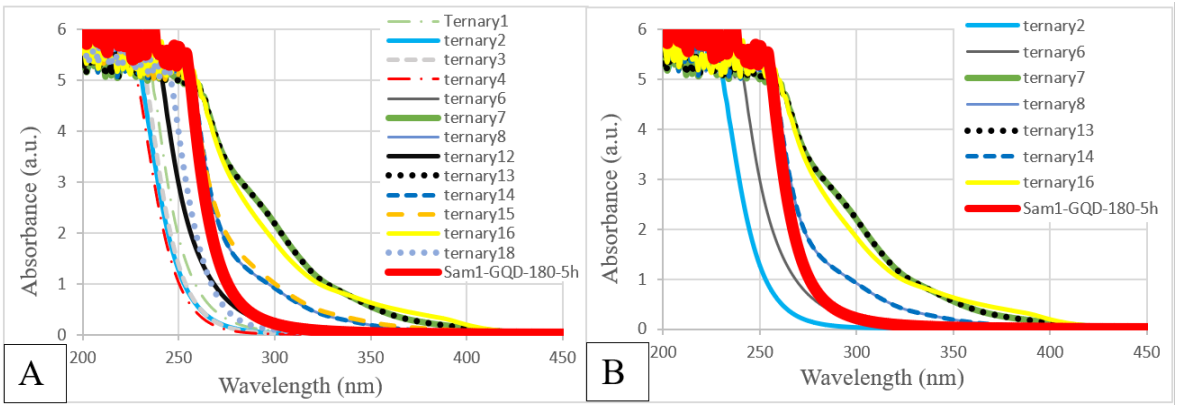

Figure 25. (A) UV-vis spectrum of all Ternary experiments with Sam1-GQD-180-5h and (B) chosen Ternary samples for TEM analysis alongside Sam1-GQD-180-5h

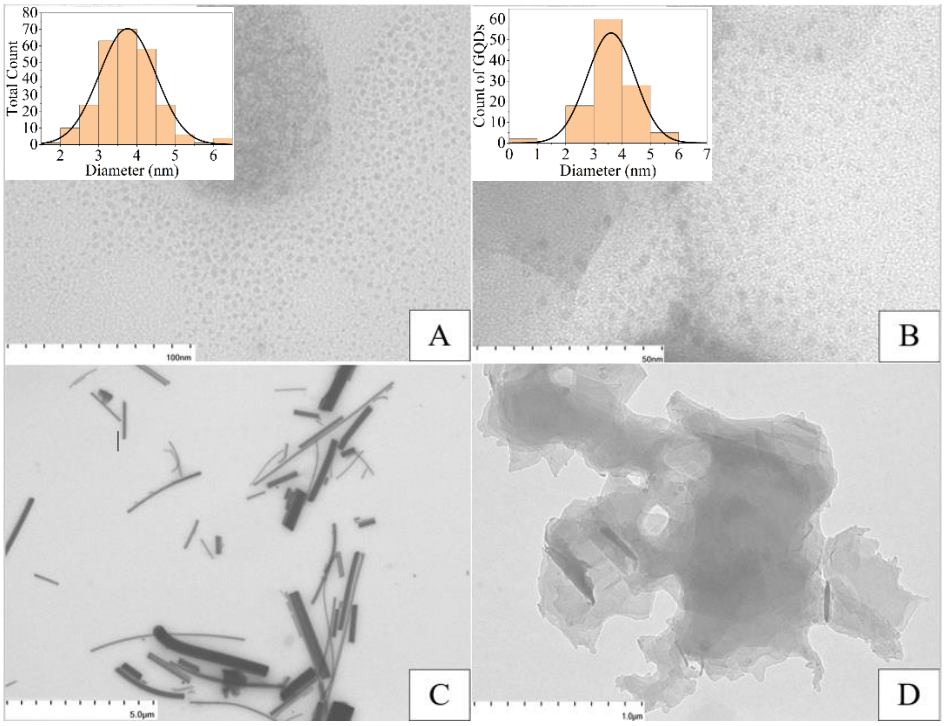

Figure 26. TEM images of (A) Ternary 2, (B) Ternary 6, (C) Ternary 7, and (D) Ternary 8

All these 7 samples could be divided into 3 groups based on what was found in TEM images. In the first group were included the experiments that clearly showed the presence of dispersed GQDs i.e., Ternary 2 and Ternary 6 (Figure 26 (A) and (B)) as well as the more water there are present the fewer by-products/aggregations are produced. The second group included the experiment that did have GQDs attached to the surface of nanofibers i.e., Ternary 7 (Figure 26 (C)). Lastly, the third group consisted of experiments that had only aggregations i.e., Ternary 8, Ternary 13, Ternary 14, and Ternary 16 (Figure 26 (D)). Based on these results I could say that GQDs are produced when there is no NaOH present or only little amount of NaOH is added. Otherwise, the synthesis will produce Nanofibres or aggregations (Figure 27).

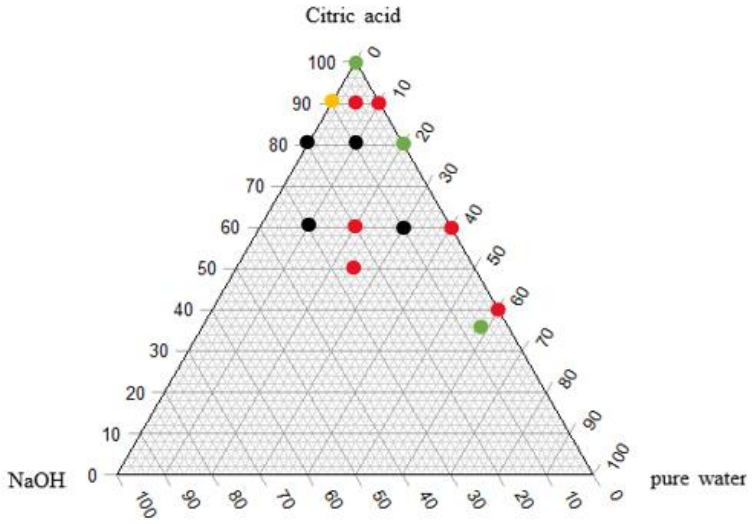

Figure 27. Gibbs/Ternary diagram where can be seen compositions of performed synthesizes (all dots) and those that were put through TEM analysis (black, green, and yellow dots)

As could be seen in Figure 27 yellow dot indicates synthesis that did have GQDs attached on the surface of nanofibers in TEM images, the green dot indicates synthesizes that did have GQDs in TEM images, the black dot indicate synthesizes that did have only aggregations in TEM images, and red dot which indicates synthesizes that did not go through TEM analysis. In my estimations, the total mass of NaOH divided by the total mass of pure water needs to be between 0 and 1/6 to produce GQDs otherwise synthesis will go out of control resulting in aggregation. On the other hand, nanofibers are produced around the Ternary 7 composition. The synthesizes that had a composition where the total mass of NaOH divided by the total mass of Pure water was between 0 and 1/6 were further studied using Fluorescence spectroscopy (Figure 28).

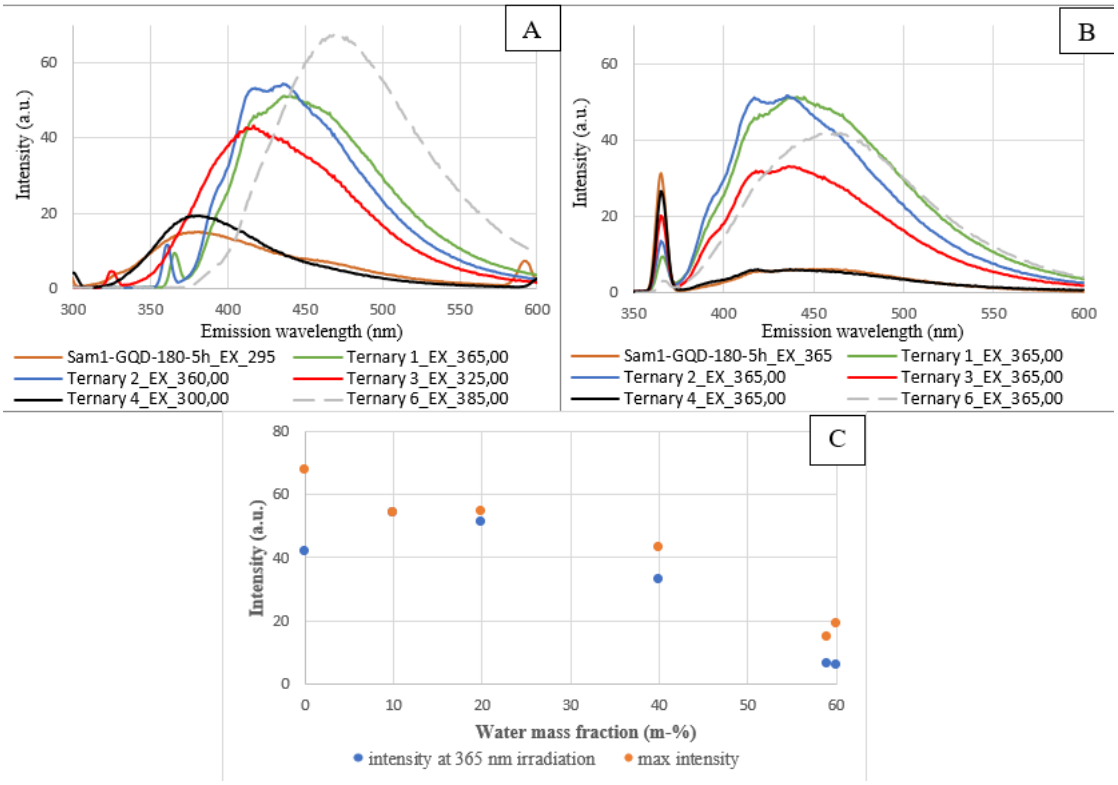

Figure 28. The PL spectrum of the (A) strongest intensity of the experiment, (B) the PL spectrum at the specific excitation wavelength (365 nm), and (C) a summary of maximum and at 365 nm irradiation intensities based on water mass fraction

In Figure 28 (A) and (B) are PL spectrum plots, where was used excitation wavelength that gives the strongest emission intensity and where was used excitation wavelength of 365 nm respectively while the (C) plot is a summary of intensities of (A) and (B) plots based on used mass fraction of water. From all three plots can be seen the same behavior as what was observed in the previous two chapters e.g., the transition state was affected. Another interesting observation is in the intensity growth. Less water present in the synthesis the stronger the maximum intensity as well as the excitation wavelength needed for maximum PL and the emission wavelength produced at constant irradiation (365 nm) become longer. This is a good indication that the particle size of GQDs has grown. Performed TEM analysis also affirms particle size growth statement because in performed histograms the average GQDs diameter of Ternary 2 (80m-% of CA and 20m-% of water) is 3.5±0.5 nm and the average GQDs diameter of Ternary 6 (100m-% of CA) is 4±1 nm (Figure 29 (A-B)). On the other hand, Sam1-GQD-180-5h (59m-% of water, 6m-% of NaOH, and 35m-% of CA) has the biggest amount of water, and by logic needs to produce the smallest GQDs. In reality, the GQD synthesis is accelerated by NaOH. This component compensates for the water effect by producing larger GQDs which have an average diameter of 4.5±1.5 nm (Figure 29

(C)). Contrary to expectations synthesis goes out of control by producing by-products because the amount of NaOH is not optimal. The presence of by-products is seen in big amounts of aggregations in TEM images.

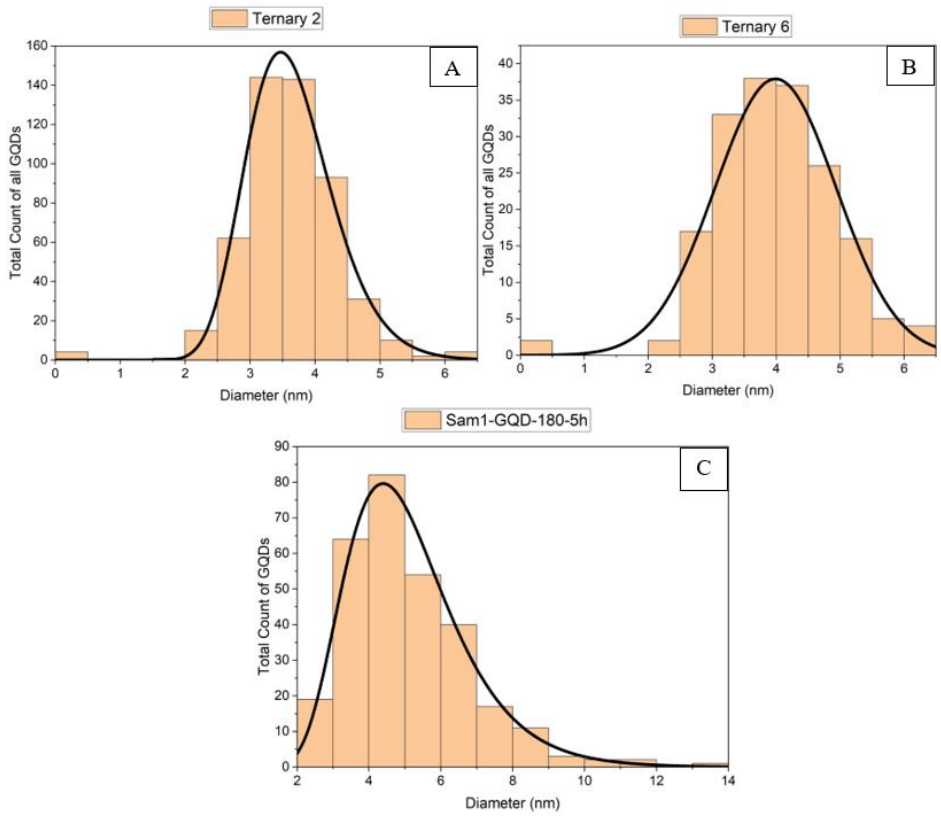

Figure 29. Histograms of all GQDs found in TEM images for (A) Ternary 2, (B) Ternary 6, and (C) Sam1-GQD-180-5h

In these histograms can be seen how water and NaOH affect the size distribution of GQDs. In chapter 4.1 was mentioned that the presence of water creates distance between precursors slowing their reaction which makes it possible to produce GQDs that are uniform in size if (A) and (B) of Figure 29 are compared. Interestingly, Elfers (2012) has stated that adding water in little amounts can speed up chemical reactions tremendously because hydrogen is starting material or reactant in hydrogenolysis, or the hydrogenation process takes place [46]. So, it could be said that the composition where water was not added did react with bigger conversion-producing clusters because with the condensation reaction some water was also produced.

4.1.5 Different Precursor Results

D(+)-glucose anhydrous was chosen as the alternative for CA because glucose not only has a molecular structure that resembles that of CA but compared to CA it does not have an acidic branch/functional group (-COOH) in the middle and in edges of the molecular structure. In my opinion, this acidic branch of CA makes the molecule asymmetrical (Figure 30 A) and less effective for GQDs production i.e., harder to destroy oxygen double bond located in the carboxyl group. In addition, glucose has a symmetrical molecular structure without many carbonyl groups (=O) while the molecule has many hydroxyl groups (Figure 30 B) making it easier to react and produce GQDs.

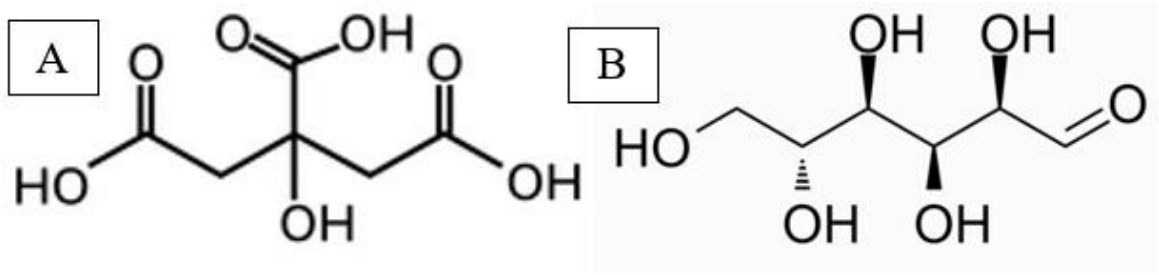

Figure 30. Molecular structure difference between Citric acid (A) [43] and D-Glucose (B) [47]

Previously determined optimal synthesis conditions for CA were used with the glucose (i.e., 180°C for 5 hours) to see how these parameters will affect GQDs formation when the precursor is changed. After carrying out synthesizes described in chapter 3.2.1.4 there was seen black solution under visible light (Figure 31).

Figure 31. The hydrothermal treatment product using D(+)-Glucose anhydrous as the precursor

Hossain et. al. 2016 mentioned that exfoliation of graphene sheets produces GQDs of different sizes while the process turns the solution black colored. As can be seen from the product shown in Figure 31 its color does resemble what was described by Hossain et. al. (2016). TEM images, however, did not confirm the formation of GQD from D(+) Glucose as a precursor. Only clusters of graphene sheets (Figure 32) and nanofibers (not shown) have been detected.

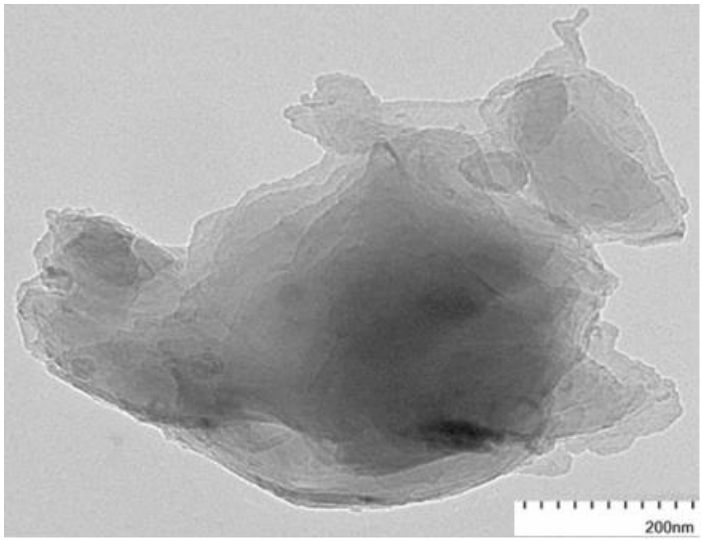

Figure 32. TEM image of synthesis where glucose was used as the precursor

This indicates that minimum one of the three vectors, namely composition, reaction temperature, and reaction time, was not optimal which led to synthesis that is out of the control and producing by-products. Looking from the other perspective, this indicates that optimizing compositions and lowering reaction temperature can produce GQDs making it more economical and effective than synthesis using CA as the precursor. For that more experiments need to be done.

4.2 Microwave-Assisted Synthesis Results

It is a known fact that irradiation affects molecular bonds directly making them reactive while conventional thermal heating affects the first vessel and then molecules. That is why I performed experiments using microwave irradiation to find out if the microwave oven can intensify GQDs synthesis and make it more effective and economic compared to conventional heating. In this experiment, it was not possible to use a closed vessel which

means that water in the solution will evaporate while remnants overflow the vessel or if water is not present at the start of the process chemicals will burn. Based on this it was decided to use 2 different compositions “Ternary 2 and Ternary 13” which after water evaporation had the composition of “Ternary 6 and Ternary 7” respectively. After carrying out synthesizes, as described in chapter 3.3, it was found that the mixture that has the composition of Ternary 2 was unsuccessful as the products burned. For the successful experiment that had a solution composition of Ternary 13 was performed TEM analysis (Figure 33) to see how irradiation does affect GQDs formation with the presence of NaOH while water is constantly evaporating.

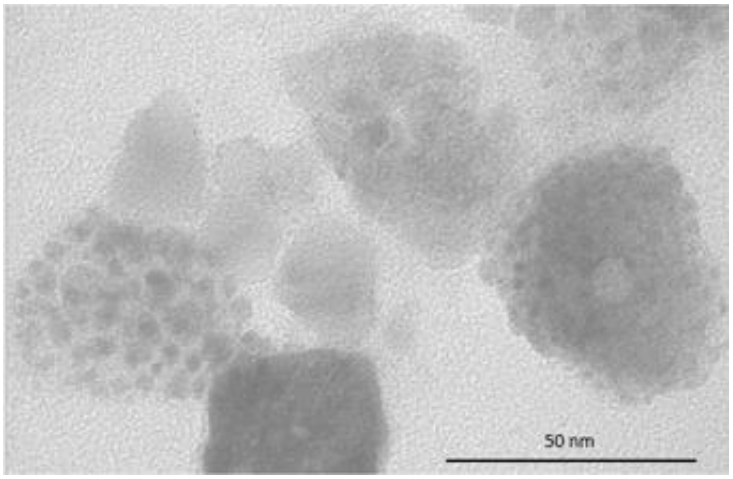

Figure 33. TEM image of Ternary 13 synthesis product after irradiation for 1 minute

As can be seen from Figure 33 TEM image, the presence of NaOH have a reverse effect in microwave irradiation synthesis compared to the thermal heating process (Figures 17 and 26). The reason why the effect is reversed is behind water evaporation. Because water evaporates the distance between precursors will be shortened which will as the result lead to the production of by-products (or burning). That is why the reaction needs to happen fast so that GQDs are produced while water is still present which can be done with the presence of NaOH. The optical properties of this successfully synthesized sample were further studied by UV-vis-NIR spectrophotometer and compared with Sam1-GQD-180-5h and Sam1-GQD-190-5h (Figure 34).

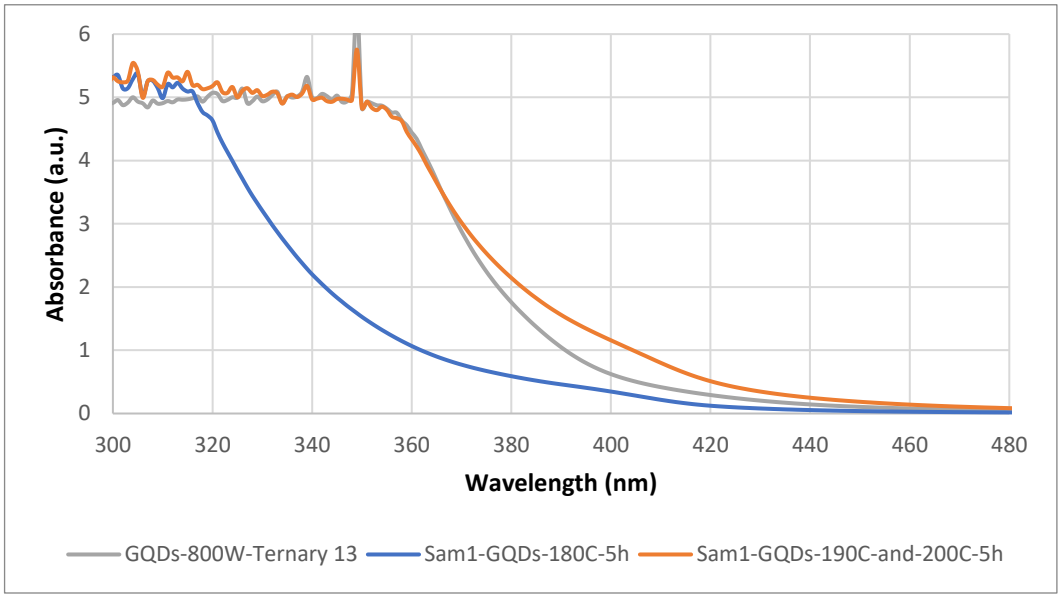

Figure 34. UV-vis spectrum of Ternary 13 experiment with Sam1-GQD-180-5h Sam1-GQD-190-5h

In Figure 34 can be seen that 1-minute irradiation in a microwave using 800W have stronger absorption than Sam1-GQD-180-5h and a little weaker than Sam1- GQD-190-5h. Meaning that there are more products with PL properties than in Sam1-GQD-180-5h. This indicates that microwave irradiation is more economical and effective than conventional thermal heating for several hours in high temperatures from the energy consumption perspective as well as production/precursor conversion perspective. It also was indicated through TEM images that synthesis using the microwave is more controllable than conventional thermal heating. The reason is behind reaction time which is less than 1 minute resulting that components do not have time to react further and aggregate. This proves that the irradiation process is the preferable method of GQDs production if the composition of the components, reaction time, and irradiation energy (W) are optimized for the open vessel as well as for the closed vessel.

5 Conclusions

GQDs have been successfully synthesized through thermal heating methods using different temperatures, compositions, and reaction times. This research achieved the objective of finding optimal conditions to synthesize GQDs of the wanted size in big quantities with fewer side reactions.

In research was found that temperature directly affects the amount of the precursor carbonization and the end form it will take. At the temperature of 180^{o}C, the GQDs were produced and the reaction is faster than in lower temperatures. It was found that if the temperature is too high then the reaction will go out of control by producing Nanofibres (190^{o}C) or aggregations (200^{o}C). The presence of water creates distance between precursors, making them react slower and producing fewer by-products. Moreover, the more there is water present the more uniform in size GQDs are (80m% CA and 20m% water produced 3.5±0.5nm GQDs) compared to synthesis without water (100m% CA produced 4±1nm GQDs) which is good from an efficiency perspective. Theoretically, the more there is water the fewer by-products are produced and if synthesis time is prolonged then it will produce GQDs with bigger diameters without by-products. In addition, it was proved that NaOH does accelerate the reaction and compensates for the water effect (59m% water, 6m% NaOH, and 35m% CA produced 4.5±1.5nm GQDs). TEM images showed that GQDs are produced if NaOH:water is between 0 to 1:6. The more there is NaOH present the bigger GQDs particles are but their quantity will be fewer, meaning that the reaction goes out of control by producing aggregations.

It is a known fact that GQDs have different characteristics depending on their size, shape, and functionality. This research focused on finding optimal conditions to synthesize GQDs with specific sizes and shapes so that it could be possible in the future to produce GQDs with the wanted characteristics (functionalized if needed) in big quantities for different applications. In the future, temperature, composition, and reaction time need to be studied more. The reason is that different compositions have different optimal conditions and these vectors will greatly impact the production of GQDs with specific sizes and shapes.

Different precursors have also been tested namely glucose. But in the same synthesis conditions, it did burn which indicates that composition, temperature, and reaction time were

not optimal making it hard to make conclusions. Moreover, the microwave irradiation method was also tested to see if conventional thermal heating can be intensified and make it more economical and effective. Experiments showed that it is possible to produce GQDs more economically and effectively because the reaction time in the experiment was only 1 minute under an 800W power supply. But the vessel, used in the synthesis, could not be closed which is why it is hard to compare with the conventional thermal heating method.

References

(1) Mansuriya, B. D.; Altintas, Z. Graphene Quantum Dot-Based Electrochemical Immunosensors for Biomedical Applications. Materials **2019**, 13 (1), 96. https://doi.org/10.3390/ma13010096.

(2) Younis, M. R.; He, G.; Lin, J.; Huang, P. Recent Advances on Graphene Quantum Dots for Bioimaging Applications. Front. Chem. **2020**, 8, 424. https://doi.org/10.3389/fchem.2020.00424.

(3) Raja, I. S.; Song, S.-J.; Kang, M. S.; Lee, Y. B.; Kim, B.; Hong, S. W.; Jeong, S. J.; Lee, J.-C.; Han, D.-W. Toxicity of Zero- and One-Dimensional Carbon Nanomaterials. Nanomaterials **2019**, 9 (9), 1214. https://doi.org/10.3390/nano9091214.

(4) Campuzano, S.; Yáñez-Sedeño, P.; Pingarrón, J. M. Carbon Dots and Graphene Quantum Dots in Electrochemical Biosensing. Nanomaterials **2019**, 9 (4), 634. https://doi.org/10.3390/nano9040634.

(5) Singh, V. K.; Yadav, P. K.; Chandra, S.; Bano, D.; Talat, M.; Hasan, S. H. Peroxidase Mimetic Activity of Fluorescent NS-Carbon Quantum Dots and Their Application in Colorimetric Detection of H2O2 and Glutathione in Human Blood Serum. J. Mater. Chem. B **2018**, 6 (32), 5256–5268. https://doi.org/10.1039/C8TB01286E.

(6) Fu, Z. D.; Cui, Y. S.; Zhang, S. Y.; Chen, J.; Yu, D. P.; Zhang, S. L.; Niu, L.; Jiang, J. Z. Study on the Quantum Confinement Effect on Ultraviolet Photoluminescence of Crystalline ZnO Nanoparticles with Nearly Uniform Size. Appl. Phys. Lett. **2007**, 90 (26), 263113. https://doi.org/10.1063/1.2750527.

(7) Bailey, R. E.; Nie, S. Alloyed Semiconductor Quantum Dots: Tuning the Optical Properties without Changing the Particle Size. J. Am. Chem. Soc. **2003**, 125 (23), 7100–7106. https://doi.org/10.1021/ja035000o.

(8) Barman, M. K.; Patra, A. Current Status and Prospects on Chemical Structure Driven Photoluminescence Behaviour of Carbon Dots. J. Photochem. Photobiol. C Photochem. Rev. **2018**, 37, 1–22. https://doi.org/10.1016/j.jphotochemrev.2018.08.001.

(9) Fetzer, J. C. THE CHEMISTRY AND ANALYSIS OF LARGE PAHs. Polycycl. Aromat. Compd. **2007**, 27 (2), 143–162. https://doi.org/10.1080/10406630701268255.

(10) Zhang, L.; Yin, L.; Wang, C.; lun, N.; Qi, Y.; Xiang, D. Origin of Visible Photoluminescence of ZnO Quantum Dots: Defect-Dependent and Size-Dependent. J. Phys. Chem. C **2010**, 114 (21), 9651–9658. https://doi.org/10.1021/jp101324a.

(11) Waris, R.; Rembert, M. A.; Sellers, D. M.; Acree, W. E.; Street, K. W.; Fetzer, J. C. Polycyclic Aromatic Hydrocarbon Solute Probes. Part II. Effect of Solvent Polarity on the Fluorescence Emission Fine Structures of Coronene Derivatives. The Analyst **1989**, 114 (2), 195. https://doi.org/10.1039/an9891400195.

(12) Difference between ammonia and urea on nitrogen doping of graphene quantum dots - ScienceDirect. https://www.sciencedirect.com/science/article/abs/pii/S0927775720312966 (accessed 2022-05-03).

(13) Liu, C.; Zhang, F.; Hu, J.; Gao, W.; Zhang, M. A Mini Review on PH-Sensitive Photoluminescence in Carbon Nanodots. Front. Chem. **2021**, 8.

(14) Zhu, S.; Zhang, J.; Qiao, C.; Tang, S.; Li, Y.; Yuan, W.; Li, B.; Tian, L.; Liu, F.; Hu, R.; Gao, H.; Wei, H.; Zhang, H.; Sun, H.; Yang, B. Strongly Green-Photoluminescent Graphene Quantum Dots for Bioimaging Applications. Chem. Commun. **2011**, 47 (24), 6858. https://doi.org/10.1039/c1cc11122a.

(15) Ju, J.; Chen, W. Synthesis of Highly Fluorescent Nitrogen-Doped Graphene Quantum Dots for Sensitive, Label-Free Detection of Fe (III) in Aqueous Media. Biosens. Bioelectron. **2014**, 58, 219–225. https://doi.org/10.1016/j.bios.2014.02.061.

(16) Ananthanarayanan, A.; Wang, Y.; Routh, P.; Sk, M. A.; Than, A.; Lin, M.; Zhang, J.; Chen, J.; Sun, H.; Chen, P. Nitrogen and Phosphorus Co-Doped Graphene Quantum Dots: Synthesis from Adenosine Triphosphate, Optical Properties, and Cellular Imaging. Nanoscale **2015**, 7 (17), 8159–8165. https://doi.org/10.1039/C5NR01519G.

(17) Qu, D.; Sun, Z.; Zheng, M.; Li, J.; Zhang, Y.; Zhang, G.; Zhao, H.; Liu, X.; Xie, Z. Three Colors Emission from S,N Co-Doped Graphene Quantum Dots for Visible Light H $_2$ Production and Bioimaging. Adv. Opt. Mater. **2015**, 3 (3), 360–367. https://doi.org/10.1002/adom.201400549.

(18) Kundu, S.; Yadav, R. M.; Narayanan, T. N.; Shelke, M. V.; Vajtai, R.; Ajayan, P. M.; Pillai, V. K. Synthesis of N, F and S Co-Doped Graphene Quantum Dots. Nanoscale **2015**, 7 (27), 11515–11519. https://doi.org/10.1039/C5NR02427G.

(19) Jablonski Diagram. Wikipedia; 2021.

(20) Tang, L.; Ji, R.; Li, X.; Bai, G.; Liu, C. P.; Hao, J.; Lin, J.; Jiang, H.; Teng, K. S.; Yang, Z.; Lau, S. P. Deep Ultraviolet to Near-Infrared Emission and Photoresponse in Layered N-Doped Graphene Quantum Dots. ACS Nano **2014**, 8 (6), 6312–6320. https://doi.org/10.1021/nn501796r.

(21) Manikandan, A.; Chen, Y.-Z.; Shen, C.-C.; Sher, C.-W.; Kuo, H.-C.; Chueh, Y.-L. A Critical Review on Two-Dimensional Quantum Dots (2D QDs): From Synthesis toward Applications in Energy and Optoelectronics. Prog. Quantum Electron. **2019**, 68, 100226. https://doi.org/10.1016/j.pquantelec.2019.100226.

(22) Hantoko, D.; Yan, M.; Prabowo, B.; Susanto, H. Preparation of Empty Fruit Bunch as a Feedstock for Gasification Process by Employing Hydrothermal Treatment. Energy Procedia **2018**, 152, 1003–1008. https://doi.org/10.1016/j.egypro.2018.09.107.

(23) Microwave heating drying sterilization mechanism. https://www.langfengmetallic.com/news-in-company/microwave-heating-drying-sterilization-mechanism.html (accessed 2022-04-10).

(24) Water-Based Graphene Exfoliation. Hielscher Ultrasonics. https://www.hielscher.com/water-based-graphene-exfoliation.htm (accessed 2022-04-10).

(25) Tian, P.; Tang, L.; Teng, K. S.; Lau, S. P. Graphene Quantum Dots from Chemistry to Applications. Mater. Today Chem. **2018**, 10, 221–258. https://doi.org/10.1016/j.mtchem.2018.09.007.

(26) Ghorai, S.; Roy, I.; De, S.; Dash, P. S.; Basu, A.; Chattopadhyay, D. Exploration of the Potential Efficacy of Natural Resource-Derived Blue-Emitting Graphene Quantum Dots in Cancer Therapeutic Applications. New J. Chem. **2020**, 44 (14), 5366–5376. https://doi.org/10.1039/C9NJ06239D.

(27) Achee, T. C.; Sun, W.; Hope, J. T.; Quitzau, S. G.; Sweeney, C. B.; Shah, S. A.; Habib, T.; Green, M. J. High-Yield Scalable Graphene Nanosheet Production from Compressed Graphite Using Electrochemical Exfoliation. Sci. Rep. **2018**, 8 (1), 14525. https://doi.org/10.1038/s41598-018-32741-3.

(28) Hossain, S. T.; Wang, R. Electrochemical Exfoliation of Graphite: Effect of Temperature and Hydrogen Peroxide Addition. Electrochimica Acta **2016**, 216, 253–260. https://doi.org/10.1016/j.electacta.2016.09.022.

(29) Haque, E.; Kim, J.; Malgras, V.; Reddy, K. R.; Ward, A. C.; You, J.; Bando, Y.; Hossain, Md. S. A.; Yamauchi, Y. Recent Advances in Graphene Quantum Dots:

Synthesis, Properties, and Applications. Small Methods **2018**, 2 (10), 1800050. https://doi.org/10.1002/smtd.201800050.

(30) Tyurnina, A. V.; Tzanakis, I.; Morton, J.; Mi, J.; Porfyrakis, K.; Maciejewska, B. M.; Grobert, N.; Eskin, D. G. Ultrasonic Exfoliation of Graphene in Water: A Key Parameter Study. Carbon **2020**, 168, 737–747. https://doi.org/10.1016/j.carbon.2020.06.029.

(31) Massabeau, S.; Riccardi, E.; Rosticher, M.; Valmorra, F.; Huang, P.; Tignon, J.; Kontos, T.; Dhillon, S.; Ferreira, R.; Mangeney, J. THz Band Gap in Encapsulated Graphene Quantum Dots. In 2018 43rd International Conference on Infrared, Millimeter, and Terahertz Waves (IRMMW-THz); IEEE: Nagoya, 2018; pp 1–2. https://doi.org/10.1109/IRMMW-THz.2018.8509964.

(32) Linkov, P.; Samokhvalov, P.; Grokhovsky, S.; Laronze-Cochard, M.; Sapi, J.; Nabiev, I. Selection of the Optimal Chromatography Medium for Purification of Quantum Dots and Their Bioconjugates. Chem. Mater. **2020**, 32 (21), 9078–9089. https://doi.org/10.1021/acs.chemmater.0c03195.

(33) Robertson, J. D.; Rizzello, L.; Avila-Olias, M.; Gaitzsch, J.; Contini, C.; Magoń, M. S.; Renshaw, S. A.; Battaglia, G. Purification of Nanoparticles by Size and Shape. Sci. Rep. **2016**, 6 (1), 27494. https://doi.org/10.1038/srep27494.

(34) Bai, L.; Ma, X.; Liu, J.; Sun, X.; Zhao, D.; Evans, D. G. Rapid Separation and Purification of Nanoparticles in Organic Density Gradients. J. Am. Chem. Soc. **2010**, 132 (7), 2333–2337. https://doi.org/10.1021/ja908971d.

(35) Guerra-Rodríguez, L.; Muñoz, M.; González, E.; Matas, C.; Carbajal Arizaga, G. Citric Acid Removal from Aqueous Solution with Layered Aluminum Hydroxide Crystals. Iran. J. Chem. Chem. Eng.-Int. Engl. Ed. **2018**, 37, 153–161.

(36) Shakeri, B.; Meulenberg, R. W. A Closer Look into the Traditional Purification Process of CdSe Semiconductor Quantum Dots. Langmuir **2015**, 31 (49), 13433–13440. https://doi.org/10.1021/acs.langmuir.5b03584.

(37) Dheyab, M. A.; Aziz, A. A.; Jameel, M. S.; Noqta, O. A.; Khaniabadi, P. M.; Mehrdel, B. Simple Rapid Stabilization Method through Citric Acid Modification for Magnetite Nanoparticles. Sci. Rep. **2020**, 10 (1), 10793. https://doi.org/10.1038/s41598-020-67869-8.

(38) Large Scale Purification of Colloidal Quantum Dots. AZoM.com. https://www.azom.com/article.aspx?ArticleID=13661 (accessed 2022-06-18).

(39) Lim, H.; Woo, J. Y.; Lee, D. C.; Lee, J.; Jeong, S.; Kim, D. Continuous Purification of Colloidal Quantum Dots in Large-Scale Using Porous Electrodes in Flow Channel. Sci. Rep. **2017**, 7 (1), 43581. https://doi.org/10.1038/srep43581.

(40) Kim, D.; Park, H. K.; Choi, H.; Noh, J.; Kim, K.; Jeong, S. Continuous Flow Purification of Nanocrystal Quantum Dots. Nanoscale **2014**, 6 (23), 14467–14472. https://doi.org/10.1039/C4NR04351K.

(41) Tam, T. V.; Hong, S. H.; Choi, W. M. Facile Synthesis of Cysteine–Functionalized Graphene Quantum Dots for a Fluorescence Probe for Mercury Ions. RSC Adv. **2015**, 5 (118), 97598–97603. https://doi.org/10.1039/C5RA18495A.

(42) Mikalsen, R. F. Hydrothermal Synthesis of Materials for Intermediate Band Solar Cells, 2013.

(43) Citric Acid. Wikipedia; 2022.

(44) Sang, S.; Yang, S.; Guo, A.; Gao, X.; Wang, Y.; Zhang, C.; Cui, F.; Yang, X. Hydrothermal Synthesis of Carbon Nano-Onions from Citric Acid. Chem. – Asian J. **2020**, 15 (21), 3428–3431. https://doi.org/10.1002/asia.202000983.

(45) Yang, S.; Zhu, C.; Mo, R.; He, P.; Sun, J.; Di, Z.; Kang, Z. H.; Yuan, N.; Ding, J.; Ding, G.; Xie, X. A New Mild, Clean and High-Efficient Method for Preparation of Graphene Quantum Dots without by-Products. J. Mater. Chem. B **2015**, 3. https://doi.org/10.1039/C5TB01093D.

(46) In chemical reactions, water adds speed without heat. https://news.wisc.edu/in-chemical-reactions-water-adds-speed-without-heat/ (accessed 2022-04-10).

(47) D-(+)-Glucose (CAS 50-99-7). https://www.caymanchem.com/product/23733 (accessed 2022-04-10).